Proceedings of the XVII ECSMGE-2019
Geotechnical Engineering foundation of the future
ISBN 978-9935-9436-1-3

doi: 10.32075/17ECSMGE-2019-1112

XVII European Conference
ECSMGE 2019
Reykjavik
on Soil Mechanics
and Geotechnical Engineering

Recent developments in laboratory testing of geomaterials with emphasis on imaging

Développements récents de la géomécanique expérimentale de laboratoire : focus sur l'imagerie

Gioacchino Viggiani & Alessandro Tengattini
Univ. Grenoble Alpes, CNRS, Grenoble INP, 3SR, F-38000 Grenoble, France

ABSTRACT: This paper presents a review of some recent technical developments and scientific accomplishments in laboratory experimental testing of geomaterials – with a special focus on imaging. Full-field techniques such as x-ray and neutron tomography have had a particular impact over the last two decades, and allowed the understanding of the micro scale processes ultimately driving the behavior at the macroscopic scale. Two other very recent, advanced experimental tools are briefly discussed: rheography and diffraction. These two modern techniques have shown increasing potential to further expand the portfolio of possibilities of experimental geomechanics, by expanding temporal resolution, and giving direct access to intra-granular strains, respectively. This contribution concludes by outlining the broader impact that this panoply of techniques has had and is expected to have in geomechanics and geotechnics at large.

RÉSUMÉ: Cet article présente quelques développements techniques et réalisations scientifiques récents en matière d'expérimentation en laboratoire sur les géomatériaux – avec un accent particulier sur l'imagerie. Les techniques de mesure de champs telles que la tomographie à rayons x et la tomographie à neutrons ont eu un impact important au cours des deux dernières décennies et ont permis de comprendre les processus à l'échelle micro qui déterminent finalement le comportement des sols à l'échelle macroscopique. L'article examine également deux autres méthodes expérimentales avancées, la rhéographie et la diffraction. Ces deux techniques modernes ont le potentiel pour élargir davantage la gamme des possibilités expérimentales en géomécanique, en améliorant la résolution temporelle, et en permettant la mesure des déformations intra-granulaires, respectivement. Finalement, cet article souligne l'impact plus large que cette panoplie de techniques a eu et devrait avoir en géomécanique et en géotechnique en général.

Keywords: Experimental geomechanics; full-field methods; tomography; x-rays; neutrons; review paper

1 INTRODUCTION

During the last few decades, laboratory experimental geomechanics has experienced a tremendous – and perhaps unprecedented – leap forward, thanks to major technological advances along with a matching computational power. Besides the availability of new and powerful tools, the increased intertwining of neighboring domains in material science has enabled the diffusion of techniques previously unknown in soil and rock mechanics, *e.g.*, nanoindentation (Daphalapurkar *et al*. 2011, Hu & Zongjin 2015) and diffraction (Hall *et al*. 2018) – to mention but two.

Of particular interest and impact are the so-called non-contact measurement techniques, which over the last two decades have passed from

relatively niche to well-established tools (*e.g.*, Hild & Espinosa 2012, Viggiani & Hall 2012). Such techniques are often referred to as *full-field*, in contrast to more conventional "point-wise" or "bulk-averaged" measurement techniques, which are based on the use of transducers positioned at the specimen boundaries.

In conventional material testing, in fact, the measured response can at best be seen to represent an overall, averaged material response. Consequently, only in the case of a perfectly homogeneous material undergoing perfectly uniform deformation will the response measured from the test reflect true material (*i.e.*, constitutive) behavior. Obviously, neither are materials truly homogeneous at the scale of a laboratory specimen, nor are boundary conditions perfect. Furthermore, even when starting from "perfectly" homogeneous conditions, processes (*e.g.*, deformation) can eventually localize into more or less narrow zones (shear and compaction bands, tensile and shear cracks or fractures) at some stage of a test. In the presence of localized strains, it is clear that the meaning of stress and strain variables derived from boundary measurements of loads and displacements is only nominal, or conventional. Measuring the full field of deformation in the specimen is in this case the only way in which test results can be appropriately interpreted.

A number of full-field techniques (thermal, wave-based, optical) have been – and are being – used in laboratory testing of soil and rock: ultrasonic tomography (*e.g.*, Hall & Tudisco 2012, Tudisco *et al*. 2015), electrical resistivity tomography (*e.g.*, Comina *et al.* 2008, 2011, Derfouf *et al.* 2019), magnetic resonance imaging (*e.g.*, Sheppard *et al.* 2003, Yu *et al*. 2019, Xu *et al.* 2019), infrared thermography (*e.g.*, Luong 1990, 2007, Salami *et al*. 2017) – to mention but a few. A remarkable example is represented by the techniques based on ionizing radiation: x-rays and neutrons. This paper will focus on these two techniques, as we believe that they are at the center of a veritable revolution in experimental soil and rock mechanics – besides, they are those that we are most familiar with. X-ray and neutron imaging have a few limitations, notably spatial and temporal resolution, and the difficulty to directly access the intra-granular strains (hence inter-granular forces). An emerging technique that can help to assess them is *diffraction* (either using x-rays or neutrons), which will also be discussed. In terms of temporal resolution, rapid processes such as granular flow would require temporal resolutions incompatible even with the most performant synchrotron – not to mention that the rotation speed required would cause centripetal forces comparable to or larger than gravity (depending on the sample size). A very recent solution to this problem is x-ray *Rheography* (Baker *et al*. 2018), which allows the direct assessment of the probability distribution of velocities at high rates.

Even with synchrotrons, the spatial resolution of x-ray imaging is not good enough for investigating the mechanics of fine-grained geomaterials (*i.e.*, clays and clay rocks) at the particle scale. However, synchrotron x-ray tomography has been successfully applied, in combination with Digital Image Correlation, to investigate strain localization in clay rocks – at a scale that is much larger than the scale of clay particles, though (Lenoir *et al*. 2007, Bésuelle & Andò 2014). To access the scale of the clay particles, a suitable technique is *Broad Ion Beaming* (BIB), which allows, when coupled with Scanning Electron Microscopy (SEM), achieving a resolution of a few nanometers. BIB is used as a "knife", to cut and expose cross-sections that are then imaged by SEM. Cross-sections with an area of a few square millimeters can be obtained, which are relatively "large" as compared to those that can be obtained with *Focused* Ion Beaming (FIB) – of only a few square micrometers. See Desbois *et al*. (2017) and references quoted therein.

The structure of this paper is as follows. The next two sections (2 and 3) give an overview of x-ray and neutron imaging, respectively. For each of these two imaging techniques, the basic physics is outlined, an historical review of their use in geomechanics is given, and finally some selected examples are presented, with particular emphasis to the more recent and promising applications. Sec-

tion 4 focuses on two comparatively new applications: diffraction and rheography. Through all these examples our aim is to present the tremendous possibilities now available and the new avenues opening up for research in geomechanics.

The paper concludes with a critical review of the impact these techniques had (or could have) on geomechanics, and a discussion about their practicality (*i.e.*, how these methods might be practically employed in a "standard" geomechanics laboratory), as well as some foreseen avenues of future development. It should be noted that in this work we adopt the broader definition of geomaterials, which besides soils and rocks also includes concrete – which after all is nothing but an artificial conglomerate.

2 X-RAY IMAGING

2.1 Fundamentals

X-rays were discovered in 1895 by W.C. Röntgen, when the radiations emitted by a vacuum tube affected a barium platinocyanide screen across the room despite the obstacles interposed. Röntgen temporarily named them using the mathematical designation (x) for something unknown. The value of this non-destructive imaging technique for medical applications was immediately recognized.

X-radiation is a form of electromagnetic radiation composed of x-rays, with wavelengths ranging from 0.01 to 10 nanometers, lying between UV and gamma rays. One common way to produce x-rays is to accelerate with sufficient energy charged particles (electrons and ions) to hit a material. The deceleration of a charged particle causes the moving particle to lose kinetic energy, which is converted into a photon (braking radiation or Bremsstrahlung), this is for example the approach used in most laboratory scanners, whereas in Synchrotrons the braking radiation is produced by magnetically undulating or deviating electrons. In both cases, the upper boundary of the emitted x-rays is defined by the energy of the incident particle. X-rays interact with the outer electron shells of the atoms through different mechanisms (*e.g.*, Compton Scattering, Refraction and Reflection, Pair Production, Rayleigh Scattering).

For geomaterials, and for the energy of x-ray radiation normally used for their investigation, the predominant mechanism is photoelectric absorption (surpassed by Compton scattering as we approach higher energies). The attenuation by absorption of the x-ray intensity I (in photons per unit area and time) along an axis z can be expressed through the Beer-Lambert law for monochromatic beam as:

$$I(z) = I_0 e^{-\mu z} \tag{1}$$

where I_0 is the initial beam intensity. The coefficient of linear absorption μ can be expressed as:

$$\mu = \left(\frac{\rho_m N_A}{M}\right)\sigma_a \tag{2}$$

where ρ_m is the material density, N_A is Avogadro's number and M the molar mass. The absorption cross-section coefficient σ_a relates the number of absorption events with the atoms per unit area. This coefficient scales roughly with the fourth power of the atomic number Z, although it presents a strong discontinuity when the work provided by the radiation becomes insufficient to eject an electron belonging to the level closer to the nucleus.

X-rays are normally detected by employing special chemical compounds, named 'scintillators' which can absorb them while emitting visible light, which is then captured by cameras sometimes with the addition of optical focusing elements.

In laboratory scanners, x-rays are often times generated in conical beams, and the detectors are composed of scintillators and detector chips right behind them. In this case, the level of zoom is determined by the relative distance between the source, detector and sample. In Synchrotrons, the x-ray beam is parallel, and the detector additionally includes optical elements (*e.g.*, camera

lenses) and the zoom is determined by the optics chosen.

These elements allow acquiring bi-dimensional projections of the attenuation to x-rays of the object, named *radiographies*. To acquire then a *tomography*, several hundred projections are acquired over a range of relative angles between object and imaging axis. So-called "reconstruction" algorithms, based on the Radon transform, are then employed to obtain a 3D matrix of absorption values, which are representative – as aforementioned – of the material density and its cross-section coefficient σ_a.

2.2 Historical perspective

The use of x-ray imaging in experimental geomechanics dates back to the 1960s. To our knowledge, the earliest examples are the works of Hamblin (1962) and Calvert & Veevers (1962) for the study of the structure of sandstones – see Figure 1. In the same period, x-ray radiography was also used in Cambridge for measuring strain fields in soil (Roscoe *et al*. 1963, Roscoe 1970). The radiographs revealed extremely interesting effects associated with local changes in the soil density, namely narrow dilation bands forming in the soil models (see Figure 2). Similar observations were made by other authors (*e.g*., Kirkpatrick & Belshaw 1968, Arthur & Dunstan 1982, Vardoulakis & Graf 1982, Bransby & Blair-Fish 1975). In all these examples, x-rays were used to obtain radiographs, *i.e*., 2D images produced by x-ray radiation on photographic plates. As explained above, radiographs represent maps of attenuation accumulated through the complete soil mass in the direction perpendicular to the image, which is related to soil density.

The above studies provided valuable qualitative information on localization patterning. However, they all suffered from two major limitations: (i) lack of quantitative data on the observed density changes, and (ii) limitation to 2D images. Both limitations are overcome by x-ray Computed Tomography (CT). The principle of CT measurement consists of recording x-ray radiographs of a specimen at many different angular positions around the object. From these different projections, a three dimensional image of the object can be reconstructed with appropriate algorithms (usually based on a back projection principle); see for example Baruchel (2000) for a thorough description of the technique. X-ray CT is therefore a non-destructive imaging technique that allows quantification of internal features of an object in 3D. First developed for medical imaging, x-ray CT is now widely used in material sciences and proved its interest in various domains of geosciences, including geomechanics (see, *e.g*., the review paper by Cnudde & Boone (2013) and the several references quoted therein).

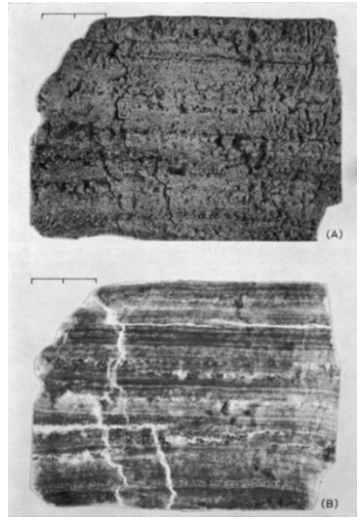

Figure 1. X-ray radiography of the structure and failure patterns in a sandstone (Calvert & Veevers 1962)

A pioneering application of x-ray CT to experimental geomechanics is due to Desrues and coworkers in Grenoble, who started from the early 1980s to use x-ray CT as a quantitative tool for experimental investigation of strain localization in sand (see Desrues *et al*. 1996, and Desrues 2004 for a review). As an example, Figure 3 shows horizontal slices through a three dimensional CT image of a specimen of dry dense Hostun sand (at a stage towards the end of a triaxial compression test). Patterns of localized density variations are

revealed as different intensities of the recorded x-ray radiation. The 3D mechanism that appears has some clear structure, which would be otherwise hidden (*i.e.*, invisible from just looking at the specimen, which to external viewing just had a barrel shape at the end of the test). Similar structures are shown in Figure 4, obtained from another triaxial test on Hostun sand (Desrues *et al*. 1996). The localization pattern in this case involves a cone and multiple sets of planes associated in pairs, each pair intersecting along a diameter at the top of the specimen. Figure 4b shows Desrues' interpretation of these patterns of localization, including a cross-section close to the top platen, and a section parallel to the axis (compare with Figure 4a).

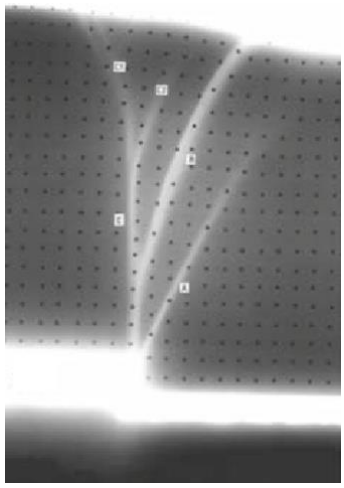

Figure 2. Dilation bands in dense sand over a displacing trapdoor observed with x-ray radiography (Roscoe et al. 1963)

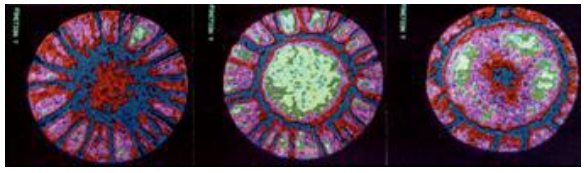

Figure 3. Horizontal slices through a CT image volume of a triaxial compression specimen of dry dense Hostun sand showing complex patterns of density variations (image was acquired near the end the test) (courtesy of J. Desrues).

Using x-ray tomography in a quantitative way requires a calibration of CT values to obtain absolute values of density or void ratio. With such a calibration, Desrues was able to show that global measurements of volume change in such tests only give an averaged picture, and in fact density variation (dilation for dense sand) occurs predominantly within the zones of localized shear. These quantitative analyses of density changes provided experimental confirmation that, for a given stress level, a unique limit void ratio is in fact reached, irrespective of the initial density of the sand being tested (the well-known concept of a critical state, as conjectured already by Casagrande & Watson (1938). However, this is only true locally, *i.e.*, within the shear zones (see Figure 4c).

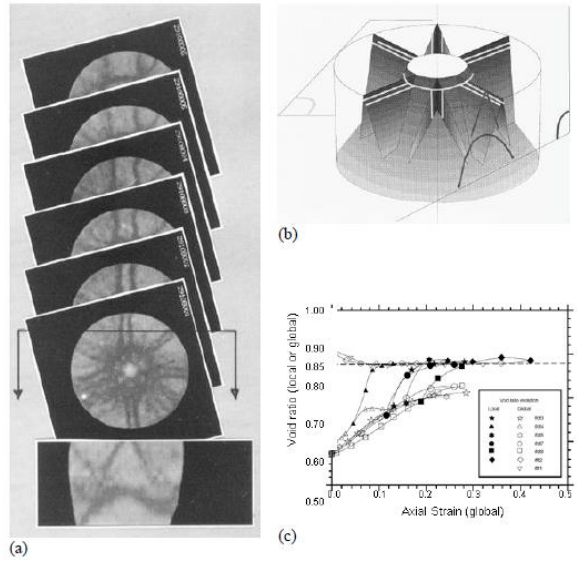

Figure 4. (a) patterns of localized density variations revealed in slices through a CT image volume of a specimen of dry dense Hostun sand near the end of a triaxial compression test (note this is a different test to Fig. 3). (b) suggested 3D interpretation of the patterns of localization in Fig. 4a. (c) local (solid symbols) and global (open symbols) variation of void ratio in loose and dense specimens of Hostun sand during triaxial compression with 60 kPa effective confining pressure (from Desrues et al. 1996).

2.3 Recent results, challenges and perspectives

This section presents recent and ongoing work where granular assemblies are deformed "in-situ" (*i.e.*, inside an x-ray tomography machine), allowing multiple states to be imaged in 3D. It is important to note that we have deliberately chosen to present examples predominantly from our personal experience at Laboratoire 3SR in Grenoble. Obviously, in so doing, we do not claim that these are necessarily the best or the most advanced examples available – they are just those that we are most familiar with. In fact, this is a technique that has become extremely popular in materials science, and in particular for granular materials, also the work of Alshibli and coworkers in the USA (*e.g.*, Druckery *et al*. 2018, just to mention their most recent publication on the subject) and the group at ANU in Australia (*e.g.*, Saadatfar *et al*. 2013) must be mentioned. The main focus of these studies is on the grain-scale investigation of shear banding, with results from triaxial tests.

The triaxial tests used in this work differ significantly from standard to allow x-ray scanning of the specimen in various stages of deformation – to this end experiments are entirely performed within the Laboratoire 3SR x-ray microtomograph. Given that the D_{50} of the grains studied is in the order of 300μm, the pixel size necessary for sufficient information for grain has been set to 15.56μm/px, meaning that an average particle will have around 20 pixels across a diameter. This choice limits the field of view and consequently the size of the specimen is reduced to 22mm height and 11mm diameter. Despite this extreme miniaturization, the specimen is composed of more than 50,000 grains of sand.

Furthermore, since x-ray tomography requires the rotation of the specimen, the steel tie bars that usually take the return force from the compression of the specimen would severely degrade the scan. To avoid this, the pressure cell (which is made in x-ray transparent Plexiglas or polycarbonate) takes this extra load. Specimens are prepared dense (through dry pluviation through a 1m tube), and are tested dry. This would normally mean that no volume changes can be measured; however these are obtained from the different 3D images. Triaxial testing is done under strain control at a strain rate of 0.1%/min, and loading is interrupted at various points during the test to scan the specimen (acquiring around a thousand radio-graphs as the specimen rotates through 360°). When loading is stopped the specimen relaxes – the majority of the relaxation happens in a few minutes after loading is stopped. Axial force and imposed displacement are measured externally.

The 3D images coming from each scan contain around 1000×1000×1600 voxels, each voxel representing a reconstructed value of x-ray attenuation (which is roughly related to density, meaning that grains have "high" and pores have "low" greyvalues). From such an image, a local field of porosity can easily be defined, for example by defining the greyvalues representing pore and grain, and measuring the average greyvalue in a suitably defined subvolume. However, the preferred technique for the low-pressure tests where grains do not break, is to define a threshold greyscale value, above which voxels are considered to be grain and below which they are considered to be pore – the value is chosen to obtain the solid volume of grains measured by weighing at the end of the test. Porosity is then easy to define in a subvolume in such an image: the volume of voids and solids are simply counted.

Binary images where the solid and void phases are defined are the starting point for the definition of individual grains: the solid phase is split into individual grains using a watershed as described in Andò *et al*. (2012a). Each grain (*i.e.*, all the voxels making up an individual grain) are then each given a unique number, and properties of these 3D sets of voxels (position, volume) can be measured. The splitting and labelling procedure is repeated for each imaged state, and since grains will not have the same unique number, labels are reconciled by tracking grains from increment to increment using a specifically developed technique called ID-Track (Andò *et al*. 2012a). Following the change in the center-of-mass of each

grain over an increment gives a very precise evaluation of the displacement of the particle (with an error less than 0.1 pixels).

The measurement of rotations is more challenging: at this resolution the grain shapes are not detailed enough for the long and short axes of the moment of inertia tensor to be stable. To overcome this problem, a discrete DIC technique has been proposed in Andò *et al*. (2012b), where tracked grains are matched based on their images – this combined with ID-Track gives the full rigid body motion of the grains.

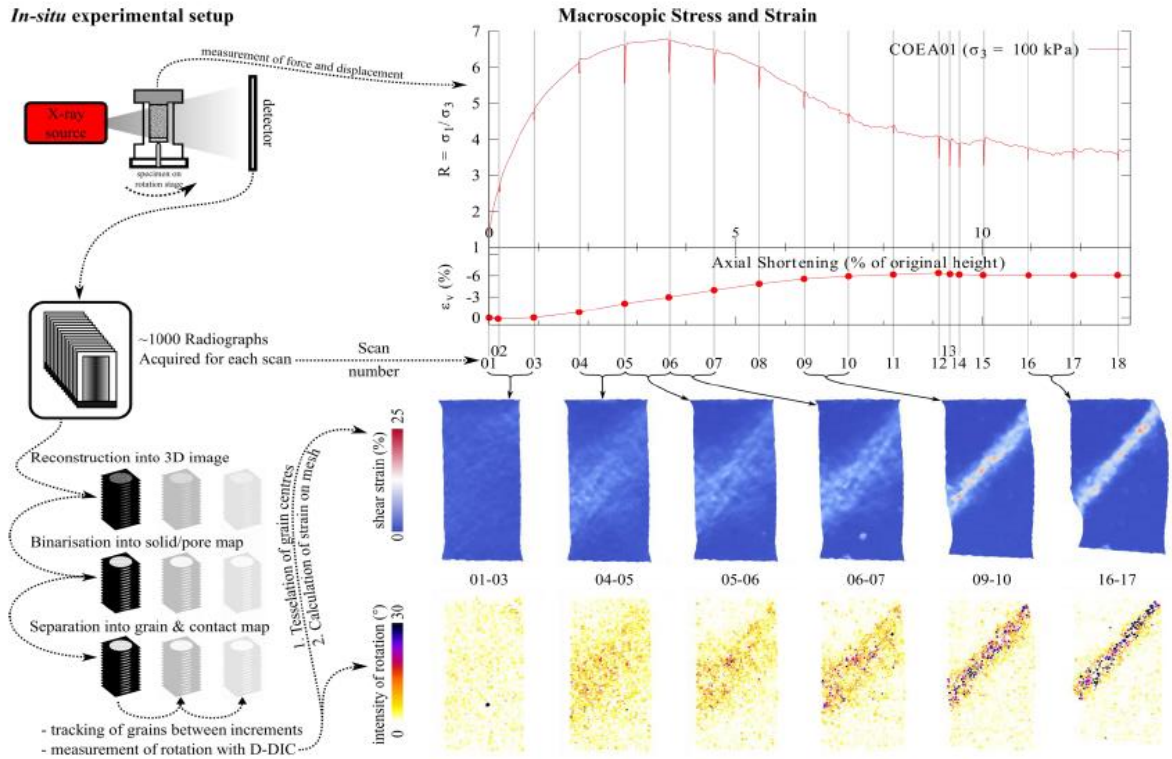

Figure 5. Illustration of the procedure for the analysis of in-situ experiments, with some highlighted results obtained on Caicos Ooids (after Andò et al. 2012a).

The measurements that can be obtained with the combination of tools detailed above are shown, for an example test, in Figure 5. In the top of the figure, a schematic of the in-situ setup is shown, along with the macroscopic measurements coming from the force and displacement measurements from the test.

In the bottom left of Figure 5, again very schematically, are shown the steps of image processing required to reconstruct a 3D image, and then to define and follow grains between imaged states, allowing measurement of their kinematics. The series of images presented at the bottom right of the figure shows vertical slices taken through the specimen at points during the test, where all grains are colored by their incremental rotations. Above these maps of discrete quantities, is a map of a continuum mechanics quantity of shear strain, measured on tetrahedra defined by tessellating grain centers.

It is clear that this kind of discrete 3D information available all the way through a mechanical test represents an experimental revolution in geomechanics. Ongoing work focuses on two areas:

solving current measurement challenges for the subject presented above, as well as elucidating new phenomena using 3D images and data processing tools similar in spirit as those presented.

The rotations of grains, as well as the shear strain maps derived from grain displacements highlight some interesting phenomena. Especially before the macro-peak, there are some interesting chains of rotating grains that can even be seen in the vertical section shown (in 3D the chains are clear to see, but unfortunately analyzing this structure in 3D as well as showing it in print also remains an open challenge). The emergence of a wide band of rotating grains that concentrates into a final shear band is also very interesting, and the grain-scale reasons for this collective behavior are doubtlessly to be found in the way that forces are transmitted from grain to grain. Looking at the grain maps, we can see that a specimen with significantly fewer grains would not have had the degrees of granular freedom in order to exhibit such a shear band. Unfortunately, having sufficient resolution to study grain kinematics does not appear, using standard tools, to offer enough to study grain-to-grain contacts, as shown in Andò *et al*. (2013) – the number of voxels describing the contact between the two objects is simply insufficient.

Problems appear both in the counting of contacts (they are systematically overestimated – see Wiebicke *et al*. (2017), as well as the extremely poor definition of their orientation.

Some work in collaboration with discrete mathematicians has allowed this measurement to be made in some idealized cases using a Random Walker (see Viggiani *et al*. 2013, the base of this algorithm is now implemented in the python toolkit skimage – see Van Der Walt *et al*. 2014), and the application of this sort of tool is part of the ongoing PhD work of M. Wiebicke, with the objective of obtaining a fabric tensor from such measurements (see Wiebicke *et al.* 2019a, 2019b).

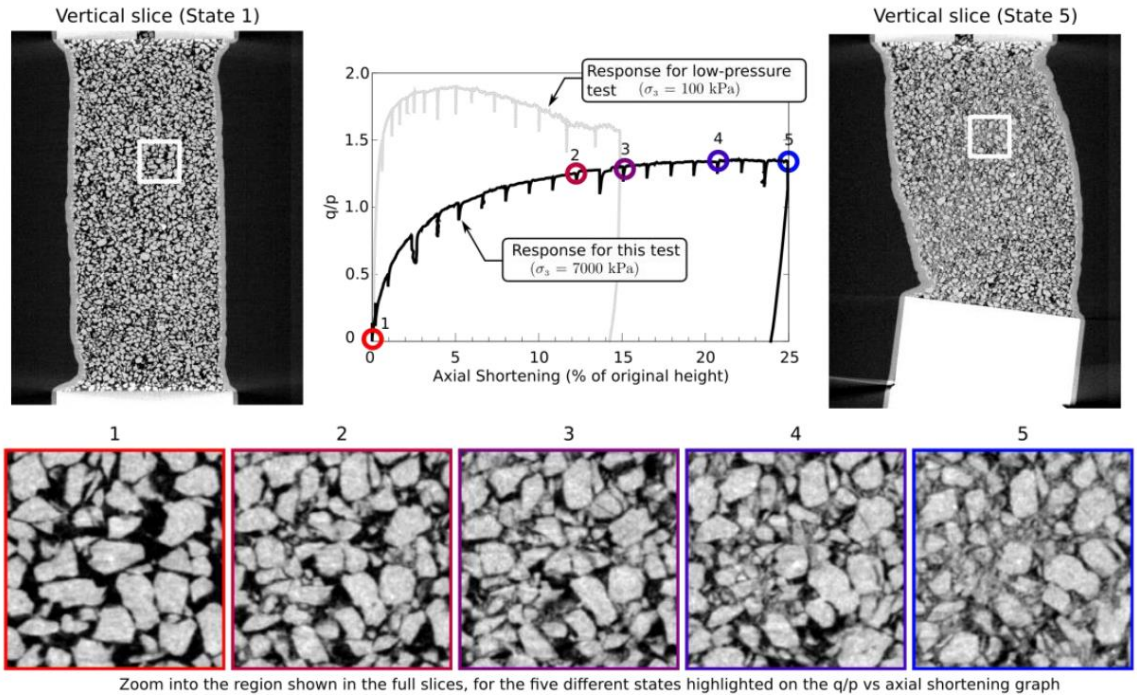

Figure 6. Some observations of grain breakage in triaxial compression of Hostun sand (after Andò et al. 2013)

Another approach to compensate for the scarcity of information is to use geometrical models to capture grain shapes, either in the style of level sets (Andrade *et al*. 2012, Kawamoto *et al*. 2018), or in the style of spherical harmonics (see Zhou *et al*. 2015). Work on all fronts is extremely important to get further in the characterization of the complex phenomenon of shear banding.

The ability to non-destructively image multiple states of a granular medium in 3D offers tremendous possibilities in the quantification of many phenomena in granular materials. In Grenoble, a number of different phenomena have been (and are being) investigated. The three-phase interaction of soil-water-air mix with a focus on the water-retention behavior of soil is an important area of focus (Kaddhour *et al*. 2018, with important work also done by other groups such as Sheel *et al*. 2008 and Higo *et al*. 2011, 2013). One of the main challenges here is the "trinarization" of such a volume to distinguish all three phases without errors; this is a particular challenge in the case of water, since its density is low compared to sand grains.

Furthermore, the quantification of cement is also an important area of research work, be it "biocemented" materials such as those produced in U.C. Davis (DeJong *et al*. 2006) which have been studied with x-ray tomography (Tagliaferri *et al*. 2011), or artificially cemented material (see Das *et al*. 2013 as well as Tengattini *et al*. 2014). Challenges here include the difficult quantification of cement and its evolution between grains (since both can be of similar grey-scale values).

One last major area of work is grain breakage (as illustrated in Figure 6), where the challenge is to quantify the process of breakage, even when particle shapes are evolving, and particle sizes are becoming small. When particles fall below the resolution of the measurement, only their average mass can be followed, and taking this into account in an algorithm is certainly a big challenge. Recent work by Karatza *et al*. (2019) propose two bespoke image analysis algorithms, which allow breakage to be tracked in 3D images of a dry granular assembly undergoing crushing, and contacts prior to breakage to be identified. Finally, it is worth noting that recent work using synchrotron based x-ray tomography indicates that even *creep* of sand can in fact be the result of rather pronounced fracturing at the individual grain scale (Andò *et al*. 2019) – see Figure 7.

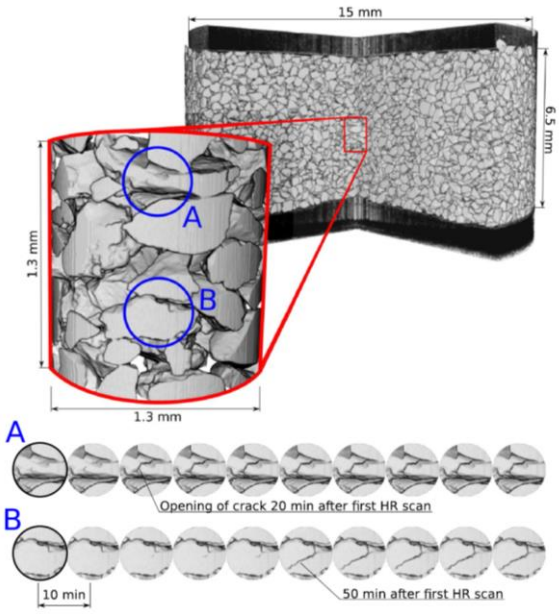

Figure 7. X-ray imaging of creep experiments on sand. Positions labelled A and B are tracked through time (after Andò et al. 2019)

3 NEUTRON IMAGING

3.1 Fundamentals

Neutrons were discovered in 1932 by J. Chadwick, while trying to understand the origin of the theoretical imbalance of the energy necessary to contain the electrons in the atom, which could not be justified by the protons alone.

Unlike x-rays, neutrons are fundamental particles which have mass and, as the name suggests, carry no electric charge. Two of the most common ways to produce neutrons is through *nuclear fission*, *e.g.*, by bombarding with one neutron a Uranium 235 atom, which splits into a Barium and a

Kripton atom plus three neutrons, with a net gain of two neutrons and about 180 MeV of energy. Alternatively, *spallation* can be adopted: protons are magnetically accelerated onto a heavy metal target as Lead, which releases about 15 to 20 neutrons per proton. The energy of neutrons is in both cases usually too high for imaging purposes, which is why they are generally slowed down by making them pass through water or heavy water tanks at low temperatures.

Unlike x-rays, neutrons interact with the nucleus of the atom, which is why they are sensitive to the different isotopes of the matter. A relevant example is provided by Hydrogen and Deuterium: they are both composed by one proton and one electron, but the latter also contains a neutron in its nucleus. As a result, their interaction with neutrons is an order of magnitude different, while being chemically and physically nearly identical. Like x-rays, neutrons interact with matter in a variety of ways, but the dominant ones in the context of geomaterials are *absorption* and *scattering*. While x-ray attenuation increases proportionally with the atomic number of the material, neutron interaction is far less obvious, as highlighted in Figure 8. One interesting example is hydrogen (and its compounds, such as water and hydrocarbons), which is nearly invisible to x-rays while highly opaque to neutrons. Similar considerations can be done for some salts (*e.g.*, the Chlorine in NaCl is highly visible), Lithium (for batteries), as well as Aluminum or Titanium, which are nearly transparent to neutrons and can thus be used to build sample environments imposing extreme conditions.

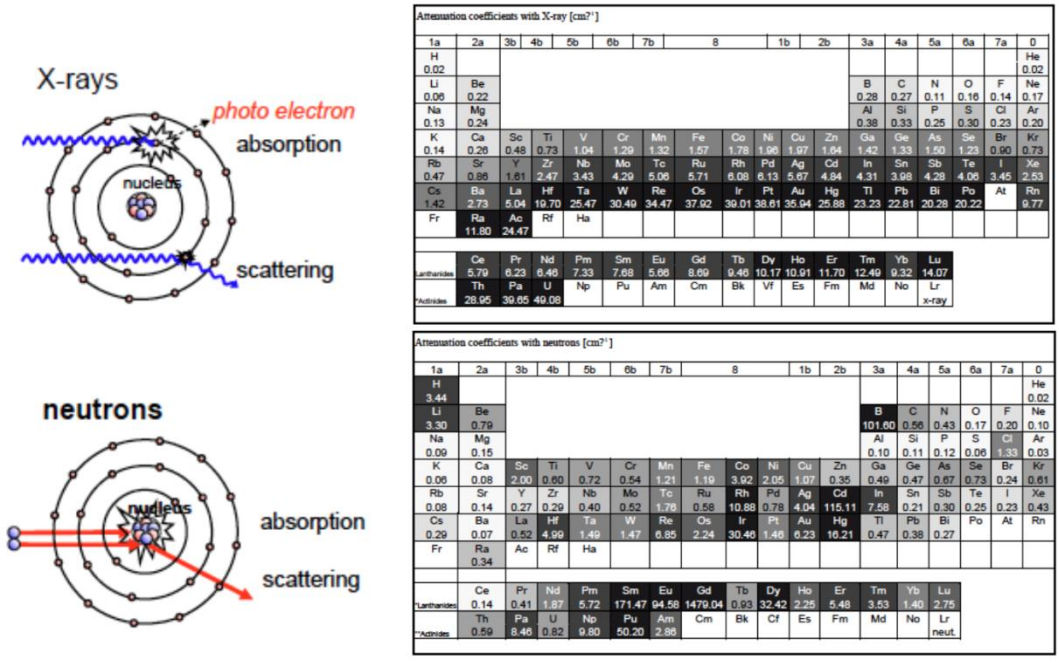

Figure 8. Interaction of x-rays and neutrons with matter: top: x-rays interact with the outer electron shells of atoms (left), which yields an increasing attenuation with increasing atomic number as highlighted by the periodic table (right). Conversely, neutrons (bottom) interact with the nuclei – hence their isotope sensitivity – and their attenuation does not depend on the atomic number.

The detection of neutrons follows the same principles as for x-rays, except that different scintillation compounds are sometimes required to convert neutrons into visible light. Producing neutrons

generally requires large-scale nuclear reactors (*e.g.*, Institut Laue-Langevin (ILL) in France, Helmholtz-Zentrum Berlin and Technische Universität München in Germany) or spallation sources (*e.g.*, European Spallation Source in Sweden and Paul Scherrer Institut in Switzerland), whereas laboratory sources are still substantially underdeveloped. The beams in these facilities are nearly parallel, so the zoom is, like in synchrotron x-rays, determined by the optical components employed. The Beer-Lambert law detailed for x-rays (Equation 1) is also generally valid for neutrons, although in some cases special attention is needed to account for the larger fraction of diffracted neutrons. The tomographic acquisition, reconstruction and data processing algorithms developed for x-rays are otherwise identical for neutrons.

3.2 Historical perspective

Neutrons were first used for geomaterials in the early 1950s, for measuring the water content in soil (Gardner & Kirkham 1952) by studying the thermalization of "fast" neutrons from a source probe. We must nonetheless wait for twenty years to see the first examples of neutron imaging applied to rocks (Subramanian & Burkhart 1973, see Figure 9), concrete (Reijonen & Pihlajavaara 1972) and soils (Wilson *et al*. 1975, Lewis & Krinitzsky 1976). The first attempt to quantitatively analyze dynamic processes in geomaterials is perhaps due to Jasti *et al*. (1987), where radiographies of water moving in rock pores were acquired. It isn't until the 1990s (Kupperman *et al*. 1990), though, that the first tomographies of a rock are reported – with the objective of characterizing water in tuff samples for permanent disposal of radioactive wastes (see Figure 10). This significant delay with respect to x-ray imaging is due to the aforementioned lower availability of neutron facilities, but also to the lower flux in most of these facilities (the most powerful of which is the one available at ILL in France), which makes the acquisition more cumbersome.

Past review papers on neutron imaging are quite broad in scope (*e.g.*, Lehmann *et al*. 2004, Winkler 2006, Banhart *et al*. 2010, Kardjilov *et al*. 2011, Kardjilov *et al*. 2018). Comparatively few review papers focus on geosciences and porous materials (Wilding *et al*. 2005, Hess *et al*. 2011, Perfect *et al*. 2014). Hereafter, we will focus on the more recent developments of neutron imaging, in particular those that are most relevant for the mechanics of geomaterials.

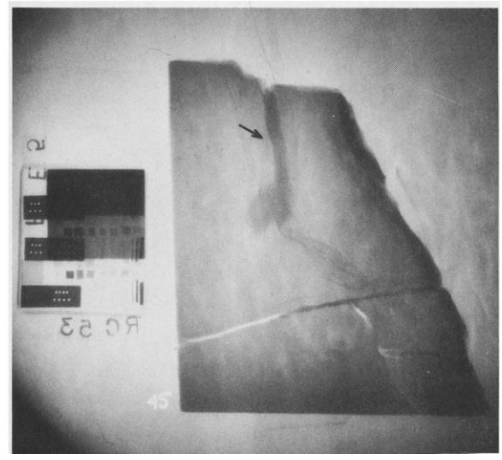

Figure 9. First neutron radiography of rock: polymer in shale (Subramanian and Burkhart 1973)

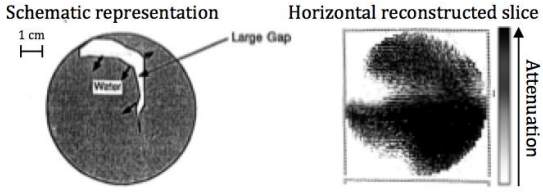

Figure 10. First neutron tomography of rock: water in tuff (Kupperman et al. 1990)

3.3 Neutron imaging for fluids

One of the key questions that neutron imaging can address is the distribution of fluids in geomaterials – thanks to the high attenuation of hydrogen to neutrons. The aforementioned pioneering work of Jasti *et al*. (1987) was followed by a number of radiographic studies of the evolving water distribution for a range of soils, rocks and concrete (de Beer *et al*. 2004, 2005, de Beer & Middleton 2006, El Abd *et al*. 2005) and even bricks

(Pleinert *et al*. 1998) and ceramics (Prazak *et al*. 1990). Some such studies (Middleton & Pàzsit 1998 and Sváb *et al*. 2000) used hydrogen isotopes such as deuterium (and the corresponding water molecule, informally named "heavy water") to obtain neutron contrast between two otherwise very similar – at least from a physico-chemical standpoint – fluids. A similar method can also be used to distinguish (heavy) water and any other fluid such as oil.

While these dynamic radiography experiments allow the observation of rapid processes of imbibition and fluid flow, their bi-dimensional nature fails to capture complex three-dimensional structures – whether intrinsic to the material or induced, for example by strain localization. In this direction, in Tudisco et *al.* (2017a) the effect of localization on fluid flow is studied by repeating a series of alternated flushes of heavy and normal water while performing the in-situ loading of a sandstone sample, highlighting the limits of radiography.

Tomography is in these cases essential, but so far the lower neutron flux available has limited most studies to static conditions, for example post-injection (Lopes *et al*. 1999, Solymar *et al*. 2003), or quasi-static conditions , *e.g.*, the determination of water retention curves in soils (Deinert *et al*. 2004, Tumlinson *et al*. 2008, Kim *et al*. 2012).

Explorations at acquisition speeds compatible with the speed of the process under investigation were generally performed at relatively low spatial resolutions. Masschaele *et al*. (2004) and Dierick *et al*. (2005), for example, acquired 10 s tomographies at a resolution of 8 pixels, or 1.5 mm.

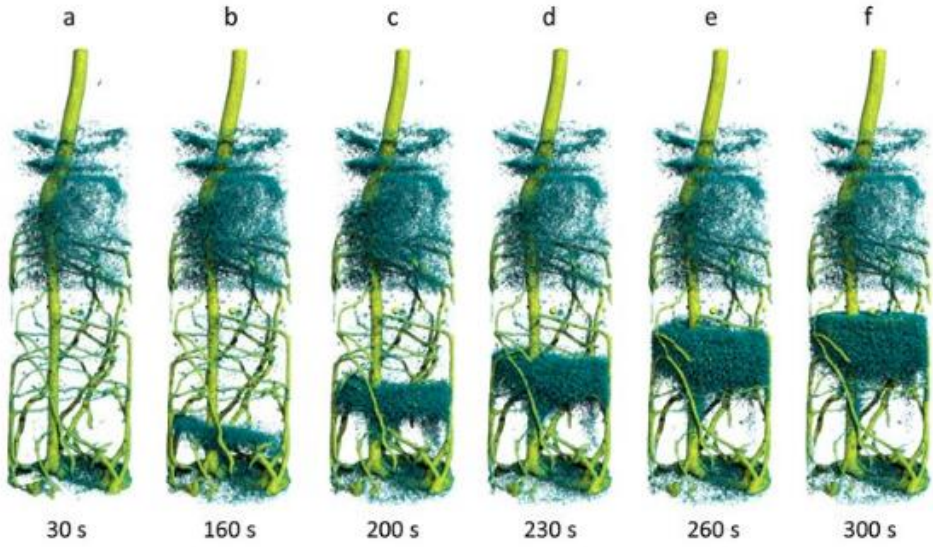

Figure 11. 3D renderings of the water uptake in Lupine roots captured through high speed (10 second) neutron tomography (after Tötzke et al. 2017)

It isn't until very recently that developments in detector technology allowed experimental campaigns that optimize resolution for a given process. A notable example is the study by Tötzke *et al*. (2017), where a series of 10 second neutron tomographies where performed on loose sand at a resolution sufficient to study the effect that lupine roots have on the hydraulic properties of granular media and most notably on the Rhizosphere (see Figure 11). A few experimental campaigns are currently being performed on rocks (sandstones and limestones) with the specific objective of investigating the influence of strain and damage localization on fluid flow (Extegarai *et al.* 2017, Lewis *et al*. 2017, Tudisco et *al*. 2019). While not

(yet) conclusive, the results obtained so far open new tantalizing perspectives.

In terms of future developments for high speed neutron tomography, the opening of imaging instruments in uniquely high flux centers (NeXT at ILL, see Tengattini *et al*. 2017, 2019) and the ongoing development of high flux centers (the European Spallation Source, ESS) will prove essential to further these efforts.

There are cases in which the experiments require relatively high confinement (cell pressure) – say several tens of MPa. This is for example the case when imaging fluid flow in concrete for understanding the durability and behavior of dams and infrastructures. In this respect, neutrons have the unique advantage over x-rays of a high penetration capability to metals, which allows the construction of high confinement vessels over sizes compatible with the intrinsic length scales of real concrete (and reinforcements), *i.e.*, several centimeters. One such testing rig, capable of withstanding 50 MPa pressure, has been recently developed by Yehya *et al.* (2018). This allowed the water flow in a concrete sample cured in heavy water to be imaged, revealing the dominant influence of local heterogeneities even at very high confinement. Besides the intrinsic interest for concrete, this also opens new interesting venues for all geomaterials at extreme conditions.

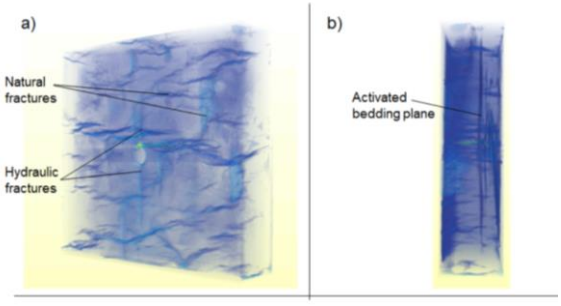

Figure 12. 3D Renderings of natural and water-injection-induced features in Marcellus Shale (after Roshankhah et al. 2018)

Comparably high pressures are for example also necessary to hydraulically fracture rocks, *e.g*, for gas extraction, to enhance geothermal energy performances as well as to study the effect of fluid in the initiation of earthquakes. A recent example of the utility of neutrons in this domain is provided by Roshankhah *et al.* (2018), where shales were hydraulically fractured *in-operando* at site conditions (equivalent to 3 km depth, in plane strain) and rapid neutron imaging allowed for following the initiation process as well as the essential role of natural shale heterogeneities such as its bedding planes (see Figure 12).

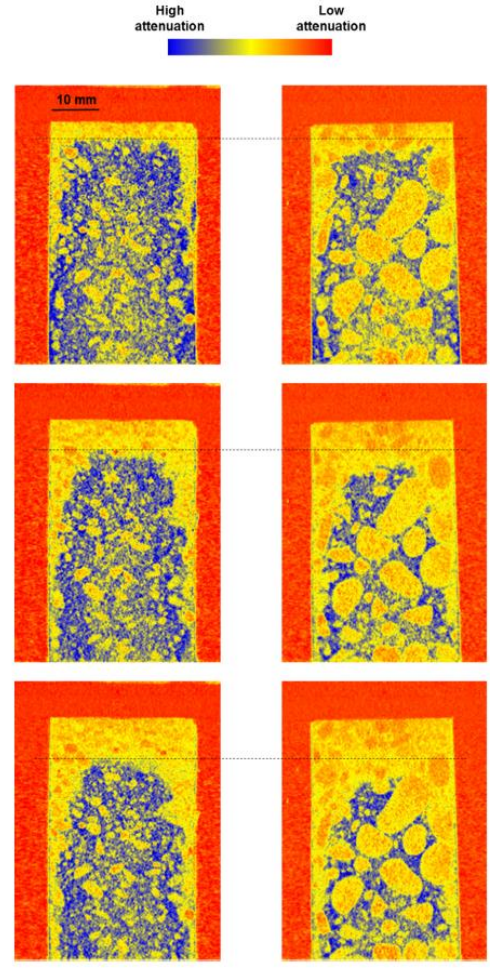

Figure 13. Vertical slices of rapid (1 minute) neutron tomographies capturing drying and moisture migration in concrete heated in operando – 4mm (left) and 8mm (right) aggregates. Top row at 38 mins, mid row at 48 mins, and bottom row at 58 mins (after Dauti et al. 2018)

A converse problem to that of fluid injection is the one of drying. A key engineering problem in this domain is moisture migration in construction materials in the event of a fire, which is at the root of explosive spalling, which in turn is a known precursor to structural collapse. In the study by Dauti *et al.* (2018), rapid (1 minute) tomographies of concrete samples heated at 500˚ were acquired. The comparison of samples with different aggregate grading revealed a significantly different hydraulic response despite a nearly identical thermal profile (Figures 13 and 14). Additionally, indicators of moisture accumulation ahead of the heating front (so far only *hypothesized* as a possible origin of spallation) were identified.

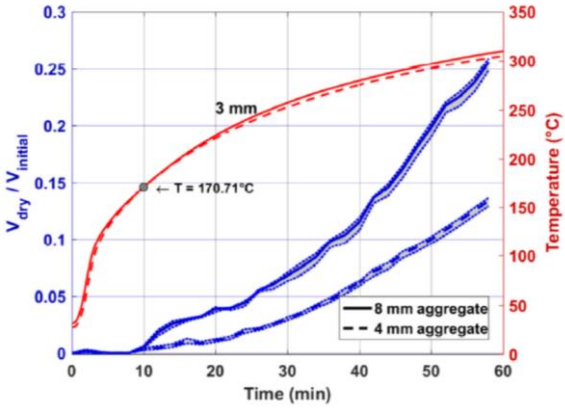

Figure 14. Comparison of the effect of aggregate size on temperature (in red) and moisture migration (in blue) as captured by neutron tomography (after Dauti et al. 2018)

All the aforementioned examples focus on the capability of neutrons to detect hydrogen and its compounds. The full potential of this technique for the broader scope of geomechanics is likely to be as of yet untapped, notably because of its less pervasive diffusion and less known potential in this domain. As highlighted in Figure 8 above in this paper (Section 3.1), a number of elements are far more (or less) visible in neutron than in x-ray imaging. So, for example, salts such as NaCl or pollutants containing Cadmium are highly visible in neutrons.

3.4 Neutron plus x-ray imaging

Besides individual advantages of x-ray over neutrons or *vice-versa*, Figure 8 highlights the extreme degree of complementarity of these two techniques. A noteworthy example of this is concrete: Figure 15 shows a scan of a concrete sample acquired with both ionizing radiations. X-rays are clearly effective in distinguishing pores from the rest of the matrix but, because of their comparable density, aggregates and mortar are barely distinguishable. Conversely, the low neutron attenuation of the SiO_2 aggregates makes them stand out with respect to the cement matrix, whereas it brings them too close to the average attenuation values of the pores to allow their straightforward segmentation. It is therefore evident that it is the *combination* of these two techniques which makes it possible to rigorously segment the essential phases. Recent theoretical developments (Tudisco *et al*. 2017b) allow not only for accurately aligning neutron and x-ray tomographies, but also for automatic segmentation of the phases – by analyzing the joint x-ray and neutron histogram. A recent paper by Roubin *et al.* (2019) presents the technical details of the algorithm proposed by Tudisco *et al*. (2017b) and applies it to neutron and x-ray tomographies of concrete (those shown in Figure 15). This yields a registered neutron image that matches the x-ray image with subpixel accuracy.

The combination of x-ray and neutron information allows also for compensating the lower neutron flux, as for example in the work by Stavropoulou *et al*. (2019a), which combines x-ray and neutrons to study the complex hydro-mechanical interactions in Callovo-Oxfordian claystone, used for the storage of nuclear pollutants. The higher speed of the x-rays and its high sensitivity to density variations can be exploited to study in 3D the evolving fracture network, whereas neutron *radiography* proves essential in determining their hydraulic origin – see Figure 16. The same authors have recently combined neutron and x-ray tomography modalities to characterize the dynamics of water absorption in Callovo-Oxfordian claystone

by comparing material deformation as well as water arrival (Stavropoulou *et al*. 2019b). Neutron and x-ray datasets are registered pairwise into a common coordinate system, meaning that a vector-valued field (*i.e*., neutron and x-ray reconstructed values) is available for each time step, essentially making this a 5D dataset. The ability to cross-plot each field into a joint histogram allows an improved identification of mineral phases in this complex material. Material deformation obtained from the application of 3D DIC on the x-ray time series data is locally compared to changes in water content available from the neutrons, opening the way towards a quantitative description of the hydro-mechanics of this process.

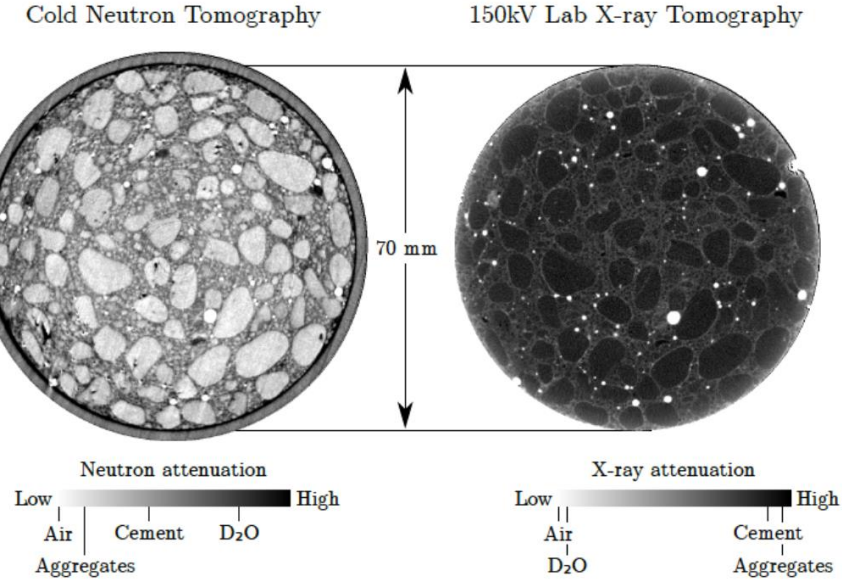

Figure 15. Example of an horizontal slice of a neutron (left) and x-ray (right) tomography of a sample of concrete, emphasizing the high complementarity of the two techniques, essential for rigorously analysing / segmenting the images (after Yehya et al. 2018). Please note that for compatibility with a white background in print, the color map has been inverted compared to the conventional for reconstructed volumes, such that low attenuation is white and high attenuation is black.

The combination of x-ray and neutron imaging for the study of geomaterials is relatively recent (*e.g.*, Kim *et al*. 2012, 2016, investigating partial saturation in granular media), albeit it is only in the last three years that some centers have started combining x-ray and neutron imaging to allow for *simultaneous* dual mode acquisitions: NeXT-Grenoble in ILL, France; ICON in PSI, Switzerland, and NeXT-NIST an NIST, USA.

Not unlike in x-ray imaging, technological developments grow along an ever growing portfolio of image processing toolboxes. While most techniques such as DIC can be used interchangeably between the two radiation types (*e.g*., Tudisco et *al*. 2015) a number of problem-specific tools for example to track fluid fronts have been developed for neutron imaging (*e.g.*, Hall 2013, Jailin *et al.* 2018, Tudisco *et al*. 2019).

4 TWO OTHER ADVANCED X-RAY TECHNIQUES

4.1 3D X-ray Diffraction (3DXRD)

A full understanding of the grain-scale mechanisms that are responsible for the mechanical be-

havior of granular soils (*i.e.*, sand) requires the ability to measure *both* the grain kinematics (particle displacements and rotations) as well as the distribution of intergranular forces through the granular assembly – in fact, it is by them that the boundary forces are transmitted through the soil mass. Valuable insight can be (and has been) gained from discrete element simulations, but these are just models and, therefore, only help in the absence of real experimental data. Photoelasticity experiments are also very insightful (*e.g.*, Majmudar & Behringer 2005), but, whilst "real", they are highly simplified – they are restricted to 2D materials.

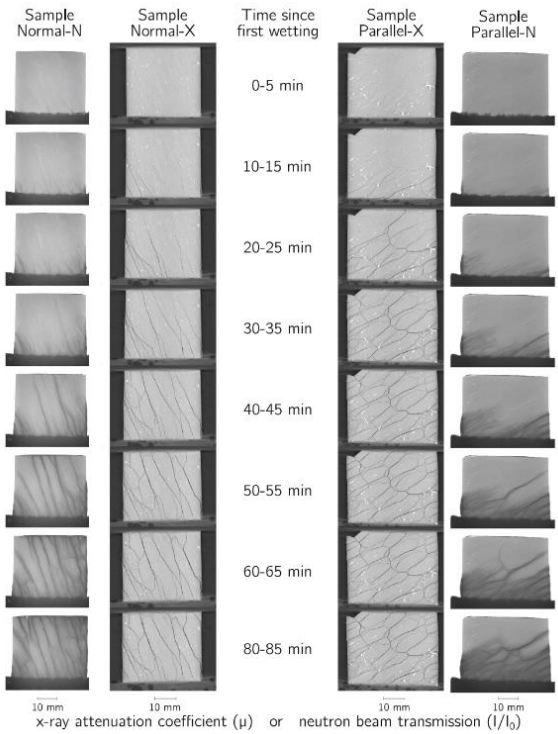

Figure 16. Comparison of x-ray tomographies and neutron radiographies of a sample of COX claystone in contact with a water reservoir, for two different orientations of the depositional layers. Water uptake is perfectly captured by neutrons, which complements the information about the fracture opening induced by it, highlighted by x-rays (after Stavropoulou et al. 2019a).

For real sand, full grain kinematics characterization has now become possible using x-ray tomography and adapted image analysis procedures – as seen in Sect. 2.3. Much fewer studies have tackled the second challenge, *i.e.*, measuring intergranular force distributions. Unfortunately, intergranular forces cannot be *directly* measured; however, they can be inferred from intragranular strains. Each grain essentially acts as a local 3D strain gauge or, for elastic deformations, a force gauge. This is in fact the basic principle of 3D x-ray diffraction (3DXRD), which has been recently proposed as a new tool that, in combination with x-ray tomography, enables force transfer networks to be studied in 3D (Hall et al. 2011, Alshibli *et al.* 2013, Cil *et al*. 2014, Hall & Wright 2015, Hurley *et al*., 2016, 2017, 2018a, Hall *et al.* 2018).

The method is based on coherent elastic x-ray diffraction, *i.e.*, the interaction of x-rays with the electron cloud around an atom leading to diffraction of waves, which interfere to produce diffraction patterns characteristic of the arrangement of atoms in the scattering crystal. The basic equation describing this scattering is Bragg's law, which can be used to infer the mean strain tensor in each individual grain from the changes in diffraction patterns – provided the position of the grain is known (see Hurley *et al*. 2017 for details).

As an example, Figure 17 shows results obtained by Hurley, Hall and coworkers (Hurley *et al*. 2017) with 3DXRD for a sample consisting of 1099 single crystal ruby grains subjected to 1D compression. In the figure, (a) is a rendered image of the sample before loading, and (b) shows the stress-strain curves using stresses based on (i) the load cell of the device and (ii) the grain stresses from the 3DXRD data. Load step/scan numbers are indicated in (b). For one specific load step (step 14), (c) shows the grain vertical stresses derived from the 3DXRD data, (d) the local vertical strains in each tetrahedron of a Delaunay triangulation, and (e) shows the contact force network.

It should be noted that all the studies cited above employed spherical single-crystal grains. However, in the very recent contribution by Hurley *et al*. (2018b), 3DXRD has been used for ex-

periments on angular quartz grains. Therefore, 3D x-ray diffraction can be now used to study the mechanics of natural granular particles, *e.g.*, sand. In our opinion, the data from this type of experiments have the potential to enable improved calibration and/or validation of models aiming to describe the details of grain-scale characteristics and deformation mechanisms.

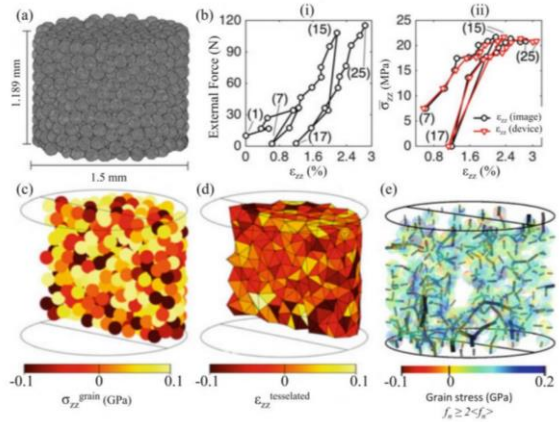

Figure 17. Example results from 3DXRD – 1D compression of a sample consisting of 1099 single crystal ruby grains. In (e) only forces greater than twice the average are shown with corresponding grains. Forces are shown as lines, centered at the corresponding contact points, scaled linearly in width and length magnitude, while grains are colored by principal stresses and given 70% transparency. Only half of the sample is shown to reveal the interior of the field (after Hall et al. 2018).

4.2 X-ray Rheography

As discussed above in the paper, one of the major limitations of tomography is temporal resolution. In most of the examples detailed in Sections 2 and 3, tomographies are acquired in quasi-static conditions. While in the most performant synchrotrons it has recently become possible to acquire images at MegaHertz rates (*e.g.*, Olbinado *et al*. 2017), their applicability in tomography for geomechanics is relatively limited. While this would allow several hundreds of tomographies per second, the centripetal forces on geomechanics-compatible samples would reach or surpass gravity, thus irrecoverably affecting the mechanical representativity of the tests.

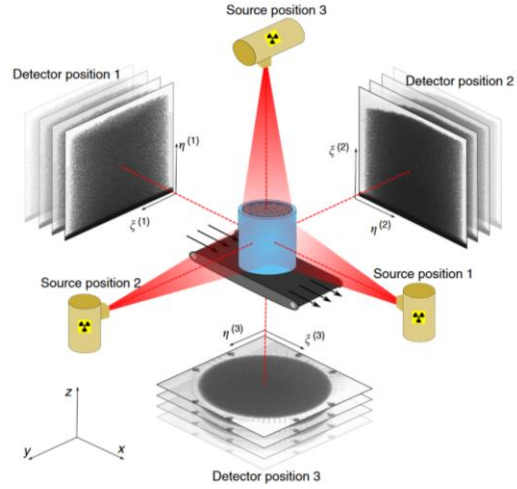

Figure 18. Schematic of the experimental set-up for rheography. Confined granular material lies inside the blue cylinder, which is sheared from below in the direction indicated. The three x-ray source positions are shown in yellow, with red indicating the approximate extent of beams, and grayscale images representing radiographic acquisition at the corresponding detector positions (after Baker et al. 2018).

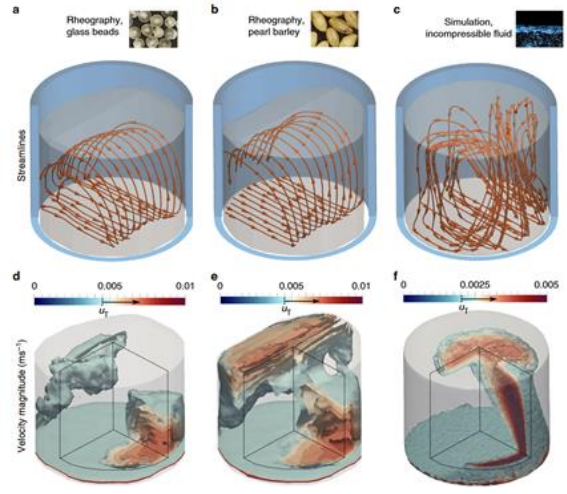

Figure 19. X-ray rheography experimental results for glass beads (a, d) and pearl barley (b, e), contrasted with the output of an incompressible Newtonian fluid simulation (after Baker et al. 2018).

A solution to this problem was recently proposed in Sydney by Einav and coworkers (Guillard *et al.* 2017, Baker *et al*. 2018). The technique was named *Rheography*, from the greek rhéō, "flow" and tomos, "slice, section". Very much like tomography, rheography allows to see the inside of the sample, however differently from tomogra-phy, it provides information about the internal flow. The scheme is illustrated in Figure 18: radiographic projections along the three cardinal axes are acquired by three x-ray source-detector pairs. Each radiography allows to evaluate the in-plane velocity. Auto- and cross-correlation functions on a regular grid can in fact be deconvolved to compute the probability density functions (PDFs) of in-plane displacements in that window. This does not nonetheless give the position of a given velocity along the x-rays although the other two source-detector pairs provide the analogous information along the other two orthogonal axes. An optimisation procedure (not unlike a Sudoku game) can then be adopted to estimate the (unique) set of velocities on a regular three-dimensional grid which can produce the distributions measured along the cardinal axes. In the work of Baker *et al*. (2018), steady state flow is imposed thanks to a conveyer belt on two granular materials with different degrees of sphericity. Representative results of the streamlines and velocity magnitudes are reported in Figure 19, revealing a highly planar flow (unlike the simulated results for a fluid), which is then successfully matched to DEM simulations.

5 DISCUSSION AND CONCLUDING REMARKS

5.1 Potential for geomechanics

Imaging techniques of the type illustrated in the previous sections allow for unprecedented observations and a renewed understanding of geomaterials and processes – as stated by Viggiani *et al*. (2014), they "allow old questions to be revisited with relatively low experimental effort yet with the promise of gaining great insight and the potential for surprising observations of unexpected structures". Furthermore, these techniques provide, when combined with appropriate image analysis tools, *quantitative* information – images are experimental *data*. As such, they open new opportunities for theoretical and computational developments. In fact, the basis for constitutive models for geomaterials has historically been phenomenology: observations at the laboratory specimen level, and establishing a correlation between stress and strain. The goal has been to fit observable experimental data (stress-strain) by making use of models that depend on material properties or variables in order to explain the observed macroscopic behavior. In our opinion, the advances in experimental geomechanics that have been discussed in this paper have the potential to transform the way macroscopic stress-strain relations are developed, treated and used in practice. The road is now open for developing and *micro-inspired (continuum) constitutive models*, equipped with measurable micro-mechanics-based variables describing the evolution of the dominant inelastic processes. In other words, it is now possible to think of models possessing a direct and clear link between the macroscopic mechanical behavior and the statistically averaged evolution of the micro-structure – see, *e.g*., the work by Tengattini *et al*. (2014) and Das *et al*. (2014).

For granular geomaterials *(i.e*., sand and sandstone), the ability to acquire 3D images with a resolution of a few microns allows the grain-scale to be experimentally accessed, and phenomena to be characterized at this scale. This kind of measurement opens many doors: to treat particles discretely and analyze their collective behavior with complex networks (*e.g*., Tordesillas *et al*., 2013), as well as discrete particle-by-particle simulations (see the recent *Level Set DEM* by Andrade and coworkers: Lim *et al*. 2016, Kawamoto *et al.* 2016, 2018). It should be noted that many open metrological questions remain, since the development of accurate and well-characterized image analysis tools is a careful procedure (see Wiebicke *et al.* 2017), however the tempting prospect of an-

swering longstanding macro-questions at the micro-scale makes the challenge worth facing.

5.2 X-rays and physical modeling

This paper has mainly discussed the application of imaging to *element testing*. However, imaging is also of interest when applied to small-scale laboratory models, *i.e.*, *physical modeling*. Physical models can be defined as "physical idealizations of all or part of an envisioned geotechnical system" (White *et al.* 2013). They may provide qualitative and quantitative insights into soil-structure interaction and geotechnical behavior – particularly where simulation by numerical methods is problematic. Given the complexity of soil constitutive behavior and the complex deformations and processes in some construction technologies, physical modeling provides a basis to assess fundamental modes of behavior in controlled conditions – a more convenient method of gaining knowledge than observing or simulating the full geotechnical system. Physical models use well-characterized soil and known boundary conditions, thus providing reliable performance data for a given idealized problem. Of course, proper application of scaling laws is vital when interpreting physical model tests. In other terms, in order to link physical model test data to a field scale prototype, correct account must be made of the influence of size and timescale effects. In general, test conditions are admittedly not representative of true field, real engineering conditions. In fact, some of the results obtained from such physical models cannot (*and should not*) be directly extrapolated to field cases. However, due to well-defined and fully known testing conditions, physical models provide valuable results, which can be used to validate theoretical solutions or numerical models.

Otani and coworkers at the University of Kumamoto have pioneered the use of x-ray imaging in physical modeling. They have studied a number of geotechnical problems, including soil arching in a reinforced embankment with a rigid pile foundation system (Eskişara *et al.* 2012), compaction grouting (Takano *et al.* 2013), laterally loaded piles (Otani *et al.* 2006), the interaction behavior between soil and face bolts in tunnels (Takano *et al.* 2006a, 2006b, 2009, 2010), and cavity generation in soils subjected to sewerage defects (Mukunoki *et al.* 2010).

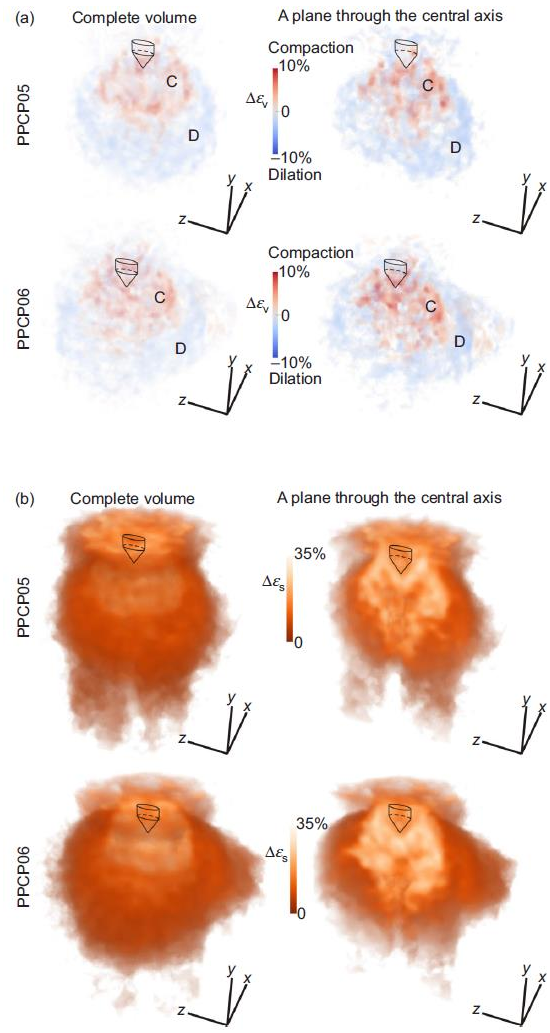

Figure 20. Incremental volumetric (a) and deviatoric (b) strains on the influence area of the cone during a 5mm penetration step of two cone penetration tests in silt (after Paniagua et al. 2013).

More recently, a few model-scale studies investigated the penetration of a probe (simulating either a penetrometer or a pile) into a soil, by means of

mini calibration chambers specifically designed to be tested inside an x-ray tomograph. Paniagua *et al*. (2013) performed cone penetration tests in silt, and used 3D DIC to quantify the evolution of displacement and strain fields in the soil. During insertion of the instrumented probe, they identified a contractant bulb of silt close to the tip of the probe surrounded by a larger bulb of dilating material – see Figure 20.

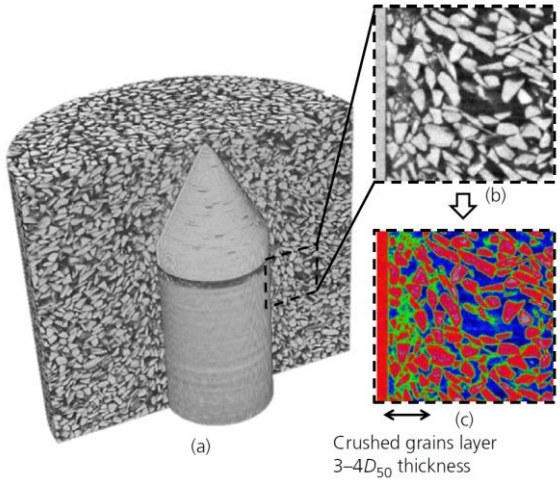

Figure 21. (a) 3D reconstructed volume after pile installation; (b) zoom on the interface; (c) detection of different phases (blue = pores, red = intact grains, and green = fines) (please note that, for practical reasons, the pile is installed from the bottom of the cell, i.e., it moves upwards) (after Doreau-Malioche et al. 2013).

The results obtained (in particular the failure mechanisms observed) shed new light on the mechanics of cone penetration in silt and consequently reflect on the interpretation of in situ CPTs. The mechanisms occurring at the grain scale at sand–pile interface under (displacement controlled) axial cyclic loading were analyzed quantitatively in a mini calibration chamber by Doreau-Malioche *et al*. (2017), again using x-ray tomography and 3D DIC. *Individual* grain kinematics and porosity evolution are followed along with the macroscopic mechanical response of the interface. Different phases in the evolution of shaft resistance during cyclic loading were observed, with a non-negligible increase of shaft resistance in the latter phase. A layer of crushed grains (about $4D_{50}$ wide) was observed at the interface – see Figure 21. The powder resulting from grain crushing is highly packed and fills the pores between intact grains. Most of particle crushing occurred during pile installation.

Alcarez-Borges *et al*. (2018) explored the use of x-ray imaging to determine the changes in bulk density associated with chalk crushing and remolding during the penetration of a mini-pile into chalk. They observed the remolded chalk annulus and measured its thickness. Thanks to 3D imaging, they found out that pile installation in the radially confined chalk specimen took place, primarily, by crushing and densification of the chalk under the pile tip.

A final thought concerns centrifuge modeling, which is widely used in geotechnical engineering research (*e.g*., the series of the International Conferences on Centrifuge Modelling in Geotechnical Engineering – ICCMGE – the last of which took place in UK in August this year). As it is well-known, the purpose of spinning physical models on the centrifuge is to increase the g-forces on the model so that stresses in the model are equal to stresses in the prototype. Geotechnical centrifuges are typically equipped with high-speed digital cameras that take on-the-fly images of one or more sides of the model. Although the experiments do not necessarily need to be in 2D, in fact the recorded photographs are (by definition) in 2D. It would be of course of extreme interest to couple geotechnical centrifuge testing and x-ray radiography – or even tomography, *i.e*, 3D (volume) imaging. Technological advances are so fast these days that one cannot exclude this is going to become possible in the near future.

5.3 Availability / practicality

A crucial issue is practicality: clearly the methods discussed in this paper are of interest, but which can reasonably be used in a "standard" geomechanics laboratory and which require large investments?

The technology of laboratory x-ray tomographs is relatively simple, accessible, and readily adoptable for geotechnical applications. In fact, in recent years there has been a rapid proliferation of laboratory x-ray imaging facilities of ever increasing quality and decreasing cost, also thanks to the large demand – recent estimates place the overall number of tomographs to several tens of thousands including hospital and industrial scanners. This broad availability, coupled with the tremendous insight they allow, is certainly at the core of the ever increasing scientific interest, also testified by the ever growing dedicated conferences and workshops (*e.g.*, the series of the biennial International Conferences on Tomography of Materials and Structures – ICTMS – the last of which took place in Australia in July this year).

When the spatial and temporal resolutions of lab scanners is insufficient, forty to fifty synchrotron sources (*e.g.*, ESRF in France, DESY in Germany, PSI in Switzerland, DIAMOND in the UK, APS in the USA, SPring-8 in Japan, and ANSTO in Australia) are also available for free, although accessing them requires the successful submission of scientific proposals which are then ranked in rather competitive rounds. However, as shown by Viggiani *et al.* (2014), insightful, high-impact findings can be made with relatively modest x-ray lab devices without having to resort to limited-access synchrotron sources.

As for neutron tomography, it clearly requires large scale facilities, such as ILL in France, TUM in Germany, ISIS in the United Kingdom, and PSI in Switzerland. Laboratory neutron scanners are also available, but their cost and flux is still not competitive with that of x-ray scanners, albeit the unique properties of neutrons still make them of great interest for some specific research applications.

6 ACKNOWLEDGEMENTS

We would like to thank all the members of our group at Laboratoire 3SR (especially Edward Andò, Pierre Bésuelle, Pascal Charrier, Jacques Desrues and Nicolas Lenoir – not to mention a number of former PhD and masters students), who are the hidden co-authors of most aspects of this paper in terms of both technical development and general philosophy. Continuous and fruitful exchange of ideas with a number of colleagues, including Steve Hall and Erika Tudisco in Lund (Sweden), Itai Einav and Benjy Marks in Sydney (Australia), Jose Andrade at Caltech (USA), and Takashi Matsushima in Ttsukuba (Japan), should also be acknowledged. Finally, we would like to acknowledge the crucial support of UGA and ILL who made possible the development of neutron imaging in Grenoble. Laboratoire 3SR is part of the LabEx Tec21 (Investissements d'Avenir - grant agreement n° ANR-11-LABX-0030).

7 REFERENCES

Alshibli, K., Cil, M.B., Kenesei, P., Lienert, U. 2013. Strain tensor determination of compressed individual silica sand particles using high-energy synchrotron diffraction. *Granular Matter*, **15**, 5, 517-530.

Alvarez-Borges, F.J., Richards, D.J., Clayton, C.R.I., Ahmed, S.I. 2018. Application of X-ray computed tomography to investigate pile penetration mechanisms in chalk. In: *Engineering in Chalk*, Proceedings of the Chalk 2018 Conference, ICE, 565-570.

Andò, E., Hall, S. A., Viggiani, G., Desrues, J., Bésuelle, P. 2012a. Grain-scale experimental investigation of localised deformation in sand: a discrete particle tracking approach. *Acta Geotechnica*, **7**, 1, 1-13.

Andò, E., Dijkstra, J., Roubin, E., Dano, C., Boller, E. 2019. A peek into the origin of creep in sand. *Granular Matter*, **21**, 11.

Andò, E., Hall, S. A., Viggiani, G., Desrues, J., Bésuelle, P. 2012b. Experimental micromechanics: grain-scale observation of sand deformation. *Géotechnique Letters*, **2**, 3, 107-112.

Andò, E., Viggiani, G., Hall, S. A., Desrues, J. 2013. Experimental micro-mechanics of granular media studied by X-ray tomography: recent results and challenges. *Géotechnique Letters*, **3**, 142-146.

Andrade, J.E., Vlahinić, I., Lim, K.W., Jerves, A. 2012. Multiscale 'tomography-to-simulation' frame-work for granular matter: the road ahead. *Géotechnique Letters*, **2**, 135-139.

Arthur, J.R.F., Dunstan, T. 1982. Rupture layers in granular media. *Proceedings of IUTAM Conference on Defects and Failure in Granular Media*, Balkema, 453-459.

Baker, J., Guillard F., Marks, B., Einav, I. 2018. X-ray rheography uncovers planar granular flows despite non-planar walls. *Nature communications* **9**, 5119.

Banhart, J., Borbély, A., Dzieciol, K., Garcia-Moreno, F., Manke, I., Kardjilov, N., Kaysser-Pyzalla, A.R., Strobyl, M., Triemer, W. 2010. X-ray and neutron imaging – complementary techniques for materials science and engineering. *Int. J. Mater. Res.*, **101**, 1069-1079.

Baruchel, J. 2000. *X-ray Tomography in Materials Science*. Paris: Editions Hermes.

Bransby, P.J., Blair-Fish, P.M. 1975. Deformation near rupture surfaces in flowing sand. *Géotechnique*, **25**, 2, 384-389.

Bésuelle, P., Andò, E. 2014. Characterization of the mechanisms of deformation at the small scale in a clay rock by in-situ X-ray micro tomography. In: *International Symposium on Geomechanics from Micro to Macro*, Cambridge, UK.

Calvert, S., Veevers, J. 1962. Minor structures of unconsolidated marine sediments revealed by x-ray radiography. *Sedimentology*, **1**, 4, 287-295.

Casagrande, A., Watson, J.D. 1938. Compaction tests and critical density investigations of cohesionless materials for Franklin Falls Dam, Merrimack Valley flood control. *Corps of Engineers, U.S. Army Engng Office*, BII-7.

Cil, M.B., Alshibli, K., Kenesei, P., Lienert, U. 2014. Combined high-energy synchrotron X-ray diffraction and computed tomography to characterize constitutive behavior of silica sand. *Nuclear Instruments and Methods in Physics Research Section B*, **324**, 11-16.

Cnudde, V., Boone, M.N. 2013. High-resolution X-ray computed tomography in geosciences: a review of the current technology and applications. *Earth-Science Reviews*, **123**, 1-17.

Comina, C., Cosentini, R.M., Della Vecchia, G., Foti, S., Musso, G. 2011. 3D-electrical resistivity tomography monitoring of salt transport in homogeneous and layered soil samples. *Acta Geotechnica*, **6**, 195-203.

Comina, C, Foti, S, Musso, G, Romero, E 2008. EIT oedometer – an advanced cell to monitor spatial and time variability in soil. *Geotechnical Testing Journal*, ASTM, **31**, 5, 404-412.

Daphalapurkar, N., Wang, F., Fu, B., Lu, H., Komanduri, R. 2011. Determination of Mechanical Properties of Sand Grains by Nanoindentation. *Experimental Mechanics*, **51**, 719-728.

Das, A., Nguyen, G.D., Einav, I. 2013. The propagation of compaction bands in porous rocks based on breakage mechanics. *Journal of Geophysical Research: Solid Earth*, **118**, 2049-2066.

Das, A., Tengattini, A., Nguyen, G.D., Viggiani, G., Hall, S.A., Einav, I. 2014. A thermomechanical constitutive model for cemented granular materials with quantifiable internal variables. Part II – Validation and localization analysis. *Journal of the Mechanics and Physics of Solids*, **70**, 382-405.

Dauti, D., Tengattini, A., Dal Pont, S., Toropovs, N., Briffaut, M., Weber, B. 2018. Analysis of moisture migration in concrete at high temperature through in-situ neutron tomography. *Cement and Concrete Research*, **111**, 41-55.

de Beer, F.C., Middleton, M.F. 2006. Neutron radiography imaging, porosity and permeability in porous rocks. *S. Afr. J. Geol*., **109**, 541-550.

de Beer, F.C., Middleton, M.F., Hilson, J. 2004. Neutron radiography of porous rocks and iron ore. *Appl. Radiat. Isot*., **61**, 487–495.

de Beer, F.C., le Roux, J.J., Kearsley, E.P. 2005. Testing the durability of concrete with neutron radiography. *Nucl. Instrum. Methods Phys. Res. A* **542**, 226-231.

Deinert, M.R., Parlange, J.-Y., Steenhuis, T., Throop, J., Ünlü, K., Cady, K.B. 2004. Measurement of fluid contents and wetting front profiles by real-time neutron radiography. *J. Hydrol*., **290**, 192-201.

DeJong, J.T., Fritzges, M.B., Nüsslein, K. 2006. Microbially induced cementation to control sand response to undrained shear. *J. Geotech. Geoenviron. Eng*., **132**, 1381-1392.

Derfouf, F., Li, Z., Abou-Bekr, N., Taibi, Z., Fleureau, J. 2019. A New Osmotic Oedometer with Electrical Resistivity Technique for Monitoring Water Exchanges. *Geotechnical Testing Journal*, **43**.

Desbois, G., Höhne, N., Urai, J.L., Bésuelle, P., Viggiani, G. 2017. Deformation in cemented mudrock (Callovo–Oxfordian Clay) by microcracking, granular flow and phyllosilicate plasticity: insights from triaxial deformation, broad ion beam polishing and scanning electron microscopy. *Solid Earth*, **8**, 291-305.

Desrues, J. 2004. Tracking Strain Localization in Geomaterials Using Computerized Tomography.

Proc. Int. Workshop on X-ray CT for Geomaterials, Kumamoto, Japan, Balkema, Lisse, The Netherlands, 15-41.

Desrues, J., Chambon, R., Mokni, M., Mazerolle, F. 1996. Void ratio evolution inside shear bands in triaxial sand specimens studied by computed tomography. *Géotechnique*, **46**, 3, 527-546.

Dierick, M., Vlassenbroeck, J., Masschaele, B., Cnudde, V., van Hoorebeke, L., Hillenbach, A. 2005. High-speed neutron tomography of dynamic processes. *Nucl. Instrum. Methods Phys. Res. A*, **542**, 296-301.

Doreau-Malioche, J., Combe, G., Viggiani, G., Toni, J.B. 2018. Shaft friction changes for cyclically loaded displacement pile: an x-ray investigation. *Géotechnique Letters*, **8**, 1-7.

Druckrey, A., Alshibli, K.A., Al-Raoush, R. 2018. Discrete Particle Translation Gradient Concept to Expose Strain Localization in Sheared Granular Materials using 3D Experimental Kinematic Measurements. *Géotechnique*, **68**, 2, 162-170.

El Abd, A.E., Czachor, A., Milczarek, J.J., Pogorzelski, J. 2005. Neutron radiography studies ofwater migration in construction porous materials. *IEEE Trans. Nucl. Sci.*, **52**, 229-304.

Eskişara, T., Otani, J., Hironaka, J. 2012. Visualization of soil arching on reinforced embankment with rigid pile foundation using X-ray CT. *Geotextiles and Geomembranes*, **32**, 44-54.

Etxegarai, M., Tudisco, E., Tengattini, A., Hall, S.A., Viggiani, G. 2017. Hydromechanical behavior of porous rock studied with neutron tomography. *Proceedings 3rd Int. Conf. on Tomography of Materials and Structures*, Lund, Sweden.

Gardner, W., Kirkham, D. 1952. Determination of soil moisture by neutron scattering. *Soil Science*, **73**, 5, 391-402.

Guillard, F., Marks, B., Einav, I. 2017. Dynamic X-ray radiography reveals particle size and shape orientation fields during granular flow. *Scientific Reports*, **7**, 8155.

Hall, S.A. 2013. Characterization of fluid flow in a shear band in porous rock using neutron radiography. *Geophysical Research Letters*. **40**, 11, 2613-2618.

Hall, S.A.,Wright, J., Pirling, T., Andò, E., Hughes, D.J., Viggiani, G. 2011. Can intergranular force transmission be identified in sand? *Granular Matter*, **13**, 251-254.

Hall, S.A., Wright, J. 2015. Three-dimensional experimental granular mechanics. *Géotechnique Letters*, **5**, 4, 236-242.

Hall, S.A., Hurley, R.C., Wright, J. 2018. Micromechanics of Granular Media Characterised Using X-Ray Tomography and 3DXRD. In: *Micro to Macro Mathematical Modelling in Soil Mechanics*, Birkhäuser, Cham, 169-176.

Hall, S.A., Tudisco, E. 2012. Full-field ultrasonic measurement (ultrasonic tomography) in experimental geomechanics. In: *Advanced experimental techniques in geomechanics*, G. Viggiani, S.A. Hall and E. Romero Eds., 103-124.

Hamblin, W. K. 1962. X-ray radiography in the study of structures in homogeneous sediments. *Journal of Sedimentary Research*, **32**, 2, 201-210.

Hess, K.-U.A., Flaws, M.J., Mühlbauer, B., Schillinger, A., Franz, M., Schulz, E., Calzada, D.B., Dingwell, Bente, K. 2011. Advances in high-resolution neutron computed tomography adapted to the earth sciences. *Geosphere*, **7**, 1294-1302.

Higo, Y., Oka, F., Kimoto, S., Sanagawa, T., Matsushima, Y. 2011. Study of strain localization and microstructural changes in partially saturated sand during triaxial tests using microfocus X-ray CT. *Soils and Foundations*, **51**, 95-111.

Higo, Y., Oka, F., Sato, T., Matsushima, Y., Kimoto, S. 2013. Investigation of localized deformation in partially saturated sand under triaxial compression using microfocus X-ray CT with digital image correlation. *Soils and Foundations*, **53**, 181-198.

Hild, F., Espinosa, H.D. (Editors) 2012. Full field measurements and identification in Solid Mechanics. Special Issue of *IUTAM Procedia*,**4**, 1-226.

Hu, C., Zongjin, L. 2015. A review on the mechanical properties of cement-based materials measured by nanoindentation. *Construction and Building Materials*, **90**, 80-90.

Hurley, R.C., Hall, S.A., Andrade, J.E., Wright, J. 2016. Quantifying interparticle forces and heterogeneity in 3D granular materials. *Physical Review Letters*, **117**, 098005.

Hurley, R.C., Hall, S.A., Wright, J. 2017. Multi-scale mechanics of granular solids from grain-resolved x-ray measurements. *Proceedings of the Royal Society A*, **473**, 0491.

Hurley, R.C., Lind, J., Pagan, D.C., Akin, M.C., Herbold, E.B. 2018a. In situ grain fracture mechanics during uniaxial compaction of granular

solids. *Journal of the Mechanics and Physics of Solids*, **112**, 273-290.

Hurley, R.C, Herbold, E.B., Pagan, D.C. 2018b. Characterization of the crystal structure, kinematics, stresses and rotations in angular granular quartz during compaction. *Journal of Applied Crystallography*, **51**(4), 021-1034.

Jailin, C., Etxegarai, M., Tudisco, E., Hall, S.A., Roux, S. 2018, Fast Tracking of Fluid Invasion Using Time-Resolved Neutron Tomography. *Transport in Porous Media*, **124**, 1, 117-135.

Jasti, J.K., Lindsay, J.T., Fogler, H.S. 1987. Flow imaging in porous mediausing neutron radiography. *SPE Annual Technical Conf. and Exhibition*, Dallas, SPE **16950**, 175-182.

Karatza, Z., Andò, E., Papanicolopulos, S.A., Viggiani, G., Ooi, J.Y. 2019. Effect of particle morphology and contacts on particle breakage in a granular assembly studied using x-ray tomography. *Granular Matter*, **21**, 44.

Kardjilov, N., Manke, I., Hilger, A., Strobl, M., Banhart, J. 2011. Neutron imaging in materials science. *Materials Today*, **14**, 248-256.

Kardjilov, N., Manke, I., Woracek, R., Hilger, A., Banhart, J. 2018. Advances in neutron imaging. *Materials Today*, **21:6**, 652-672.

Kawamoto, R., Andò, E., Viggiani, G., Andrade, J. 2016. Level set discrete element method for three-dimensional computations with triaxial case study. *Journal of the Mechanics and Physics of Solids*, **91**, 1-13.

Kawamoto, R., Andò, E., Viggiani, G., Andrade, J. 2018. All you need is shape: predicting shear banding in sand with LS-DEM. *Journal of the Mechanics and Physics of Solids*, **111**, 375-392.

Khaddour, G., Riedel, I., Andò, E., Charrier, P., Bésuelle, P., Desrues, J., Viggiani, G., Salager, S. 2018. Grain-scale characterization of water retention behaviour of sand using X-ray CT. *Acta Geotechnica*, **13**, 497-512.

Kim, F.H., Penumadu, D., Gregor J., Kardjilov, N., Manke, I. 2012. High-resolution neutron and X-ray imaging of granular materials. *J. of Geotechnical and Geoenvironmental Engineering*, **139**, 5, 715-723.

Kim, F., Penumadu, D., Kardjilov, N., Manke, I. 2016. High-resolution X-ray and neutron computed tomography of partially saturated granular materials subjected to projectile penetration. *International Journal of Impact Engineering*, **89**, 72-82.

Kirkpatrick, W.M., Belshaw, D.J. 1968. On the interpretation of the triaxial test. *Géotechnique*, **18**, 3, 336-350.

Kupperman, D.S., Hitterman, R.L., Rhodes, E., 1990. Energy dependent neutron imaging. *Review of Progress in Quantitative NDE Conference*, La Jolla, CA.

Lehmann, E.H., Vontobel, P., Kardjilov, N., 2004. Hydrogen distribution measurements by neutrons. *Appl. Radiat. Isot*., **61**, 503-509.

Lenoir, N., Bornert, M., Desrues, J., Bésuelle, P., Viggiani, G. 2007. Volumetric digital image correlation applied to X-ray microtomography images from triaxial compression tests on argillaceous rocks. *Strain, International Journal for Experimental Mechanics*, **43**, 3, 193-205.

Lewis, J.T., Krinitzsky, E.E. 1976. Neutron radiation in the study of soil and rock. In: Berger, H. (Ed.), *Practical applications of neutron radiography and gaging*. ASTM STP 586. American Society for Testing and Materials, West Conshohocken, PA, 241-251.

Lewis, M.H., Tengattini, A., Couples, G.D., Tudisco, E., Charalampidou, E.M., Hall, S.A., Etxegarai, M., Edlmann, K. 2017. Neutron radiography and tomography used to characterise water flow through a low permeability carbonate altered by experimentally induced fracture. *Proceedings 3rd Int. Conf. on Tomography of Materials and Structures*, Lund, Sweden.

Lim, K.W., Kawamoto, R., Andò, E., Viggiani, G., Andrade, J.E. 2016. Multiscale characterization and modeling of granular materials through a computational mechanics avatar: a case study with experiment. *Acta Geotechnica*, **11**, 243-253.

Lopes, R.T., Bessa, A.P., Braz, D., de Jesus, E.F.O. 1999. Neutron computerized tomography in compacted soil. *Appl. Radiat. Isot.*, 50, 451-458.

Luong, M.P. 1990. Infrared thermovision of damage processes in concrete and rock. *Engineering Fracture Mechanics*, **35**, 1–3, 291-301.

Luong, M.P. 2007. Introducing infrared thermography in soil dynamics. *Infrared Physics & Technology*, **49**, 3, 306-311.

Majmudar, T.S., Behringer, R.P. 2005. Contact force measurements and stress-induced anisotropy in granular materials. *Nature*, **435**, 1079–1082.

Masschaele, B., Dierick, M., van Hoorebeke, L., Cnudde, V., Jacobs, P. 2004. The use of neutrons and

monochromatic X-rays for non-destructive testing in geological materials. *Environ. Geol*., **46**, 486-492.

Middleton, M.F., Pàzsit, I. 1998. Neutron radiography: a technique to support reservoir analysis. *Explor. Geophys*., **29**, 512-515.

Mukunoki, T., Otani, J., Nonaka, S., Horii, T., Kuwano, R. 2010. Evaluation of Cavity Generation in Soils Subjected to Sewerage Defects using X-ray CT. In: *Advances in X-ray Tomography for Geomaterials*, J. Desrues et al. Eds, ISTE, 365-371.

Olbinado, M.P., Just, X., Gelet, J.L., Lhuissier, P., Scheel, M., Vagovic, P., Sato, T., Graceffa, R., Schulz, J., Mancuso, A., Morse, J., Rack, A. 2017. MHz frame rate hard X-ray phase-contrast imaging using synchrotron radiation. *Opt Express*, **25**(12), 13857-13871.

Otani, J., Pham, K.D., Sano, J. 2006. Investigation of failure patterns in sand due to laterally loaded pile using X-ray CT. *Soils and Foundations*, **46**, 4, 529-535.

Paniagua, P., Andò, E., Silva, M., Emdal, A., Nordal, S., Viggiani, G. 2013. Soil deformation around a penetrating cone in silt. *Géotechnique Letters*, **3**, 185-191.

Perfect, A., Cheng, C.-L., Kang, M., Bilheux, H.Z., Lamannad, J.M., Gragge, M.J., Wright, D.M. 2014. Neutron imaging of hydrogen-rich fluids in geomaterials and engineered porous media: A review. *Earth Science Reviews*, **129**, 120-135.

Pleinert, H., Sadouki, H., Wittmann, F.H. 1998. Determination of moisture distributions inporous building materials by neutron transmission analysis. *Mater. Struct*., **31**,218-224.

Prazak, J., Tywoniak, J., Peterka, F., Slonc, T. 1990. Description of transport of liquid in po-rous media—a study based on neutron radiography data. Int. J. *Heat Mass Transfer*, **33**, 1105-1120.

Reijonen, H., Pihlajavaara, S. 1972. On the determination by neutron radiography of the thickness of the carbonated layer of concrete based upon changes in water content. *Cement and Concrete Research*, **2**, 5, 607-615.

Roscoe, K.H. 1970. The influence of strains in soil mechanics, 10th Rankine Lecture, *Géotechnique*, **20** (2), 129-170.

Roscoe, K.H., Arthur, J.R.F., James, R.G. 1963. The determination of strains in soils by an x-ray method. Civ. Eng. Public Works Rev., **58**, 873-876 and 1009-1012.

Roshankhah, S., Marshall, J.P., Tengattini, A., Andò, E., Rubino, V., Rosakis, A.J., Viggiani, G., Andrade, J. 2018. Neutron Imaging: A New Possibility for Laboratory Observation of Hydraulic Fracture in Shale? *Géotechnique Letters*, **8**, 4, 1-23.

Roubin, E., Andò, E., Roux, S. 2019. The colours of concrete as seen by X-rays and neutrons. *Cement and Concrete Composites*, **104**.

Saadatfar, M., Francois, N., Arad, A., Madadi, M., Sheppard, A., Senden, T., Knackstedt, M. 2013. Grain-based characterisation and acoustic wave propagation in a sand packing subject to triaxial compression. *AIP Conference Proceedings* 1542, 571-574.

Salami, Y., Dano, C., Hicher, P.Y. 2017. Infrared thermography of rock fracture. *Géotechnique Letters*, **7**, 1-5.

Scheel, M., Seemann, R., Brinkmann, M., Di Michiel, M., Sheppard, A., Breidenbach, B., Herminghaus, S. 2008. Morphological clues to wet granular pile stability. *Nature Materials*, **7**, 189-193.

Sheppard, S., Mantleb, M.D., Sedermanb, A.J., Johnsb, M.L., Glad-den, L.F. 2003. Magnetic resonance imaging study of complex fluid flow in porous media: flow patterns and quantitative saturation profiling of amphiphilic fracturing fluid displacement in sandstone cores. *Magnetic Resonance Imaging*, **21**, 365-367.

Solymar, M., Fabricius, I., Middleton, M. 2003. Flow characterization of glauconitic sandstones by integrated dynamic neutron radiography and image analysis of backscattered electron micrographs. *Pet. Geosci*. **9**, 175-183.

Stavropoulou, E., Andò, E., Tengattini, A., Briffaut, M., Dufour, F., Atkins, D., Armand, G. 2019a. Liquid water uptake in unconfined Callovo-Oxfordian Clay-rock studied with neutron and x-ray imaging. *Acta Geotechnica*, **14**, 1, 19-33.

Stavropoulou, E., Andò, E., Roubin, E., Lenoir, N., Tengattini, A., Briffaut, M., Bésuelle, P. 2019b. Dynamics of water absorption in Callovo-Oxfordian Clayrock revealed with multimodal x-ray and neutron tomography. *Frontiers*, under review.

Subramanian, R., Burkhart, D. 1973. Determination by Neutron Radiography of the Location of Polymeric Resins Injected in Rock Fissures. *Nuclear Technology*, **17**, 2, 184-188.

Sváb, E., Balaskó, M., Kõrösi, F. 2000. Dynamic neutron radiography in petrophysical application. *Physica B*. 276–278, 916–917.

Tagliaferri, F., Waller, J., Andò, E., Hall, S.A., Viggiani, G., Bésuelle, P., DeJong, J.T. 2011. Observing strain localisation processes in bio-cemented sand using x-ray imaging. *Granular Matter*, **13**, 247-250.

Takano, D., Otani, J., Fukushige, S., Natagani, H. 2010. Investigation of interaction behavior between soil and face bolts using X-ray CT. In: *Advances in X-ray Tomography for Geomaterials*, J. Desrues et al. Eds, ISTE, 389-395.

Takano, D., Otani, J., Mukunoki, T., Date, K., Yokota, Y. 2006a. Reinforcing effect of face bolts for tunneling - application of X-ray CT and centrifuge model test. *Proceedings 17th ICSMGE*, 2469-2472.

Takano, D., Morikawa, Y., Nishimura, S., Takehana, K. 2013. Experimental study on compaction routing method for liquefiable soil using centrifuge test and X-ray tomography. *Proceedings 18th ICSMGE*, Paris, 965-968.

Takano, D., Nagatani, H., Otani, J., Mukunoki, T. 2006b. Evaluation of auxiliary method in tunnel construction using X-ray CT. *Proceedings of 6th Int. Conf. on Physical Modelling in Geotechnics*, Hong Kong, 1189-1194.

Tengattini, A., Das, A., Nguyen, G.D., Viggiani, G., Hall, S.A., Einav, I. 2014. A thermomechanical constitutive model for cemented granular materials with quantifiable internal variables. Part I – Theory. *Journal of the Mechanics and Physics of Solids*, **70**, 281-296.

Tengattini, A., Atkins, D., Giroud, B., Andò, E., Beaucour, J., Viggiani, G. 2017. NeXT-Grenoble, a novel facility for neutron and x-ray tomography in Grenoble. *Proceedings 3rd Int. Conf. on Tomography of Materials and Structures*, Lund, Sweden.

Tengattini, A., Lenoir, N., Andò, E., Giroud, B., Atkins, D., Beaucour, J., Viggiani, G. 2019. NeXT-Grenoble, the neutron and x-ray tomograph in Grenoble. U*nder review*.

Tordesillas, A., Walker, D.M., Andò, E., Viggiani, G. 2013. Revisiting localised deformation in sand with complex systems. *Proceedings of the Royal Society A: Mathematical, Physical & Engineering Sciences*, **469**, 2152, 20120606.

Tötzke, C., Kardjilov, N., Manke, I., Oswald, S.E. 2017. Capturing 3D Water Flow in Rooted Soil by Ultra-fast Neutron Tomography. *Scientific Reports*, **7**, 6192.

Tudisco, E., Hall, S.A., Charalampidou, E.M., Kardjilov, N., Hilger, A., Sone, H. 2015. Full-field measurements of strain localisation in sandstone by neutron tomography and 3D-volumetric digital image correlation. *Physics Procedia - 10th World Conf. on Neutron Radiography*. Kaestner, A. (ed.). Elsevier, **69**. 509-515..

Tudisco, E., Hall, S.A., Athanasopoulos, S., Hovind, J. 2017a. Neutron imaging and digital volume correlation to analyse the coupled hydro-mechanics of geomaterials. *Rivista Italiana di Geotecnica*, **51**:4, 60-68.

Tudisco, E., Jailin, C., Mendoza, A., Tengattini, A., Andò, E., Hall, S.A., Viggiani, G., Hild, F., Roux, S. 2017b. An extension of digital volume correlation for multimodality image registration. *Measurement Science & Technology*, **28**, 9, 095401.

Tudisco, E., Etxegarai, M., Hall, S.A., Charalampidou, E.M., Couples, G.D., Lewis, H., Tengattini, A., Kardjilov, N. 2019. Fast 4-D Imaging of Fluid Flow in Rock by High-Speed Neutron Tomography. *Journal of Geophysical Research: Solid Earth*. **124**, 4, 3557-3569.

Tudisco, E., Roux, P., Viggiani, G.M.B., Hall, S.A., Viggiani, G. 2015. Timelapse ultrasonic tomography for measuring damage localisation in geomechanics laboratory tests. *The Journal of the Acoustical Society of America*, 137 (3), 1389-1400.

Tumlinson, L.G., Liu, H., Silk, W.K., Hopmans, J.W. 2008. Thermal neutron computed tomography of soil water and plant roots. *Soil Sci. Soc. Am. J.*, **72**, 1234-1242.

Van der Walt, S., Schönberger, J.L., Nunez-Iglesias, J., Boulogne, F., Warner, J.D., Yager, N., Gouillart, E., Yu, T. & the scikit-image contributors, 2014. "scikit-image: Image processing in Python", *PeerJ* 2:e453.

Vardoulakis, I., Graf, B. 1982. Imperfection sensitivity of the biaxial test on dry sand. *Proceedings IUTAM Symposium on Deformation and Failure of Granular Materials*, Balkema, 485-491.

Viggiani, G., Andò, E., Jaquet, C., Talbot, H. 2013. Identifying and following particle-to-particle contacts in real granular media: An experimental challenge. In Powders and Grains 2013, *Proceedings of the 7th International Conference on Micromechanics of Granular Media*, AIP Publishing, 1542, 1, 60-65.

Viggiani, G., Andò, E., Takano, D., Santamarina, J.C. 2015. X-ray tomography: a valuable experimental tool for revealing processes in soils. *Geotechnical Testing Journal*, ASTM, **38**, 1, 61-71.

Viggiani, G., Hall S.A. 2012. Full-field measurements in experimental geomechanics: historical perspective,

current trends and recent results. In: *Advanced experimental techniques in geomechanics*, G. Viggiani, S.A. Hall and E. Romero Eds., 3-67.

White, D.J., Gaudin, C., Take, W.A. 2013. General report for TC104 physical modelling in geotechnics. *Proceedings 18th ICSMGE*, Paris, IOS Press, Vol. 2, 867-873.

Wiebicke, M., Andò, E., Herle, I., Viggiani, G. 2017. On the metrology of interparticle contacts in sand from x-ray tomography images. *Measurement Science and Technology*, **28**, 12, 124007.

Wiebicke, M., Andò, E., Šmilauer, V., Herle, I., Viggiani, G. 2019a. A benchmark strategy for the experimental measurement of contact fabric. *Granular Matter*, 21-54.

Wiebicke, M., Andò, E., Viggiani, G., Herle, I. 2019b. Measuring the evolution of contact fabric in shear bands with x-ray tomography. *Acta Geotechnica*, under review.

Wilding, M., Lesher, C.E., Shields, K. 2005. Applications of neutron computed tomographyin the geosciences. *Nucl. Instrum. Methods Phys. Res. A*. **542**, 290-295.

Wilson, N.E., Harms, A.A., Emery, J.J. 1975. A neutron radiographic in vitro examination of soils. *Canadian Geotechnical Journal*, **12**, 152-156.

Winkler, B. 2006. Applications of neutron radiography and neutron tomography. *Rev. Mineral. Geochem*., **17**, 459-471.

Xu, L., Li, Q., Myers, M., Chen, Q., Li, X. 2019. Application of nuclear magnetic resonance technology to carbon capture, utilization and storage: a review. *Journal of Rock Mechanics and Geotechnical Engineering*, **11**, 892-908.

Yehya, M., Andò, E., Dufour, F., Tengattini, A. 2018. Fluid-flow measurements in low permeability media with high pressure gradients using neutron imaging: Application to concrete. *Nuclear Instruments and Methods in Physics Research Section A*, **890**, 35-42.

Yu, H., Sun, D., Tian, H. 2019. NMR-based analysis of shear strength of weakly expansive clay in sodium chloride solution. *Magnetic Resonance Imaging*, 58, 6-13.

Zhou, B., Wang, J., Zhao, B. 2015. Micromorphology characterization and reconstruction of sand particles using micro X-ray tomography and spherical harmonics. *Engineering Geology*, **184**, 126-137.